



**Addis Ababa University**

**Addis Ababa Institute of Technology**

**School of Electrical and Computer Engineering**

**Design of Sliding Mode Controller Based Antilock Braking  
System of a Vehicle**

A thesis submitted to Addis Ababa Institute of Technology, School of Graduate Studies, Addis Ababa university

In partial fulfillment of the requirement for the **Degree of Master of Science in Electrical Engineering (Electrical control Engineering)**.

**By: Mekete Asmare Huluka**

**Advisor: Dr. Dereje Shiferaw Negash**

**Addis Ababa, Ethiopia**

**April, 2017**

**Addis Ababa University**

**Addis Ababa Institute of Technology**

**School of Electrical and Computer Engineering**

**Design of Sliding Mode Controller Based Antilock Braking**

**System of a Vehicle**

**By: Mekete Asmare Huluka**

APPROVED BY BOARD OF EXAMINERS

_____	_____
Chairman, Department of Graduate Committee	Signature
<u>Dr. Dereje Shiferaw Negash</u>	_____
Name of Advisor	Signature
_____	_____
Name of External Examiner	Signature
_____	_____
Name of Internal Examiner	Signature

# Acknowledgment

First of all, I would like to thank the almighty GOD, who never finishes in loving us and for the continued guidance and protection.

I would like to express my great thanks and gratitude to my advisor, Dr. Dereje Shiferaw for his spirit of an excellent teacher rather than just a supervisor, for his humanity, guidance, support and advice throughout the study.

Thank to my colleague and school of Electrical and Computer engineering dean Mr. Belete Bantealem(Msc) for his spirit of an excellent advice and helping everything throughout the study and also thanks to Mr. Bewuket Asgedom, Mr. Sintayehu Molla and Ms. Rahel Alemayehu for their supports, guide, advice and criticism.

My sincere appreciation extends to my mother, father, sister and brother for their moral support.

Finally, special thank my beloved wife Ms. Emebet Abich(Msc) for her encouragement, support and patience.

## **Declaration**

I declare that this thesis is my work and that all source materials used for this thesis have been properly acknowledged. This thesis has been submitted in partial fulfillment of the requirements for M.Sc. degree in control Engineering at Addis Ababa University. I earnestly declare that this thesis is not submitted to any other institution any where for the award of any academic degree, diploma, or certificate.

Name: Mekete Asmare Huluka

Signature:\_\_\_\_\_

Place: Addis Ababa, Ethiopia

Date of Submission:\_\_\_\_\_

This thesis has been submitted for my approval as a university advisor.

Name: Dr. Dereje Shiferaw Negash

Signature:\_\_\_\_\_

Place: Addis Ababa, Ethiopia

Date:\_\_\_\_\_

## Abstract

Anti-lock braking system (ABS) is the most common safety system in the vehicles, which works to increase the generated braking force between the tire and the road surface for enhancing passenger safety specifically related to accident avoidance. However, designing an ABS is a challenging task considering the fact that it is highly nonlinear and a time varying system. The interaction between the tires and the road surface, the dynamics of the whole vehicle and the characteristics of key components in ABS are all nonlinear and time varying. Due to the nonlinearities of the brake actuation system, robust braking control system with a faster response is required to handle even sudden, extreme variations in driving conditions with little loss of traction and steering ability.

In this thesis, out of the robust controlling mechanisms, a sliding mode controller based antilock braking system of a vehicle is introduced. The objective of this SMC based ABS is to keep the wheel slip at an ideal value so that the tire can still generate lateral and steering forces as well as shorter stopping distances in order to prevent the controlled wheel from becoming fully locked. In order to control the system based on wheel slip, a Quarter car in terms of wheel slip is modelled and the model is validated by using open loop response analysis by using MATLAB. Then a controller is designed and implemented using MATLAB. During our controller design, in order to resolve the drawback of SMC i.e. chattering, a nonlinear integral surface is defined. The designed SMC based ABS and the conventional ABS are then evaluated under dry nominal, dry concrete and dry slippery road types. And also the performance of the two systems are evaluated under three different initial vehicle velocities and the system responses are then compared in terms of wheel speed and stopping distance.

As the numerical simulation shows, on a dry nominal road, for an initial vehicle speed of 40 km/hr, the stopping distance that is obtained from the SMC based ABS and the conventional ABS are 14.5000m and 15.7080 m respectively. In the same road type, for an initial velocity of 90 km/hr, the stopping distance that is obtained from the SMC based ABS and the conventional ABS are 73.5122m and 79.6029m respectively. And also for an initial vehicle speeds of 40km/hr and 90km/hr, the braking time of the SMC based ABS is 0.11 Second and 0.39 Second faster than the conventional ABS respectively. At last, the proposed SMC based ABS achieves a robust system, minimum braking time and minimum stopping distance than the conventional ABS for all road types.

**Keywords:** Sliding Mode Control, Antilock Braking System, Sliding surface, wheel slip

# Contents

<b>Acknowledgment</b>	<b>iii</b>
<b>Declaration</b>	<b>iv</b>
<b>Abstract</b>	<b>v</b>
<b>List of Symbol</b>	<b>viii</b>
<b>List of Abbreviation</b>	<b>x</b>
<b>List of Tables</b>	<b>xi</b>
<b>List of Figures</b>	<b>xii</b>
<b>1 Introduction</b>	<b>1</b>
1.1 Background of the Study . . . . .	1
1.2 Statements of the Problem . . . . .	1
1.3 Objectives of the thesis . . . . .	2
1.4 Methodology . . . . .	2
1.5 Literature Review . . . . .	3
1.6 Scope of the thesis . . . . .	4
1.7 Outline of the Thesis . . . . .	5
<b>2 Antilock Braking System</b>	<b>6</b>
2.1 Introduction . . . . .	6
2.2 Antilock Braking System . . . . .	6
2.3 Modeling of Antilock Braking System . . . . .	10
2.3.1 Combined System . . . . .	16
2.3.2 System Dynamics In Terms of Wheel Slip . . . . .	17
<b>3 Design of Sliding Mode Controller Based Antilock Braking System</b>	<b>20</b>
3.1 Introduction . . . . .	20

3.2	Sliding Mode Control . . . . .	20
3.2.1	Sliding Surfaces . . . . .	21
3.2.2	Controller Design . . . . .	24
<b>4</b>	<b>Simulation Studies</b>	<b>28</b>
4.1	Introduction . . . . .	28
4.2	Simulation Parameters . . . . .	28
4.3	Simulation Results and Discussions . . . . .	31
<b>5</b>	<b>Conclusions, Recommendations and Future Works</b>	<b>54</b>
5.1	Conclusions . . . . .	54
5.2	Recommendations . . . . .	55
5.3	Suggestions for future works . . . . .	55
	<b>References</b>	<b>56</b>
	<b>Appendix</b>	<b>59</b>
	Appendix A: Sample MATLAB Code . . . . .	59

# List

# of

# Symbols

$\alpha$	Acceleration
$A_f$	Frontal area of the vehicle
$\alpha_w$	Wheel angular acceleration
$C_d$	Aerodynamic drag coefficient
C	Coefficient of friction
F	Total Force
$F_t$	Tire tractive force
$F_L$	Longitudnal weight transfer load
$F_v$	Wind drag force
$F_w$	Wheel viscous friction force
g	Gravitational constant
$h_{cg}$	Center of gravity height
$J_w$	Moment of inertia of wheel
L	Wheel base
l	Overall length of the vehicle
$m_t$	Mass of quarter vehicle
$m_v$	Mass of vehicle
$N_v$	Normal load
$N_w$	Number of wheels
k	Gain of the surface
$T_b$	Brake torque
$T_e$	Engine torque
$T_w$	Torque of the wheel
$u(t)$	Control input
$u_c$	Corrective control
$u_{eq}$	Equivalent control

$V$	Vehicle speed
$w$	Overall width of the vehicle
$\omega_v$	Vehicle velocity
$\omega_w$	Wheel angular Velocity
$x(t)$	State vector
$\rho$	Air density
$R_w$	Wheel radius
$\mu$	Friction coefficient
$\mu_p$	Peak value friction coefficient
$\lambda$	Wheel slip
$\lambda_p$	Peak value of wheel slip

# List

# of

# Abbreviations

ABS	Antilock Braking System
ECU	Electronic Control Unit
FLC	Fuzzy Logic Control
SMC	Sliding Mode Control
VSC	Variable Structure Control

# List of Tables

Table 4.1	system parameters [28]. . . . .	29
Table 4.2	Control parameters . . . . .	30
Table 4.3	Stopping distance and braking time Results obtained from ABS simulation with and without SMC . . . . .	31
Table 4.4	Slip results obtained from ABS simulations and with and without SMC . .	32

# List of Figures

Figure 2.1	Configuration of an ABS [16] . . . . .	8
Figure 2.2	Free body diagram of single-wheel . . . . .	8
Figure 2.3	The $\mu$ -slip curve [9] . . . . .	9
Figure 2.4	The $\mu$ -slip curve varies on different road surface [1] . . . . .	10
Figure 2.5	Wheel Dynamics . . . . .	11
Figure 2.6	Typical $\mu - \lambda$ characteristics curve[20]. . . . .	14
Figure 2.7	Curves for Different Road conditions [20]. . . . .	14
Figure 2.8	Vehicle dynamics . . . . .	15
Figure 2.9	Vehicle/road/tire one-wheel model . . . . .	19
Figure 3.1	Graphical interpretation of Equations (4.2) and (4.4) (n=2) [23] . . . . .	23
Figure 4.1	Wheel slip response of the ABS with and without SMC with various initial speeds for dry concrete road . . . . .	33
Figure 4.2	Wheel slip response of the ABS with and without SMC with various initial speeds for dry nominal road . . . . .	34
Figure 4.3	Wheel slip response of the ABS with and without SMC with various initial speeds for dry slippery road . . . . .	35
Figure 4.4	Vehicle and wheel speed response of the ABS without SMC with various initial speeds for dry concrete road . . . . .	36
Figure 4.5	Vehicle and wheel speed response of SMC based ABS with various initial speeds for dry concrete . . . . .	37
Figure 4.6	Vehicle and wheel speed response of the ABS without SMC with various initial speeds for dry nominal road . . . . .	38
Figure 4.7	Vehicle and wheel speed response of SMC based ABS with various initial speeds for dry nominal road . . . . .	39
Figure 4.8	Vehicle and wheel speed response of the ABS without SMC with various initial speeds for slippery road . . . . .	40
Figure 4.9	Vehicle and wheel speed response of SMC based ABS with various initial speeds for slippery road . . . . .	41

Figure 4.10 Stopping distance of the ABS with and without SMC with various initial speeds for dry concrete road . . . . .	42
Figure 4.11 Stopping distance of the ABS with and without SMC with various initial speeds for nominal road . . . . .	43
Figure 4.12 Stopping distance of the ABS with and without SMC with various initial speeds for slippery road . . . . .	44
Figure 4.13 Simulation graph of control input for concrete road . . . . .	45
Figure 4.14 Simulation graph of control input for nominal road . . . . .	46
Figure 4.15 Simulation graph of control input for slippery road . . . . .	47
Figure 4.16 Sliding surface of SMC based ABS with various initial speeds for dry concrete road . . . . .	48
Figure 4.17 Derivative of the sliding surface of SMC based ABS with various initial speeds for dry concrete road . . . . .	49
Figure 4.18 Sliding surface of SMC based ABS with various initial speeds for nominal road . . . . .	50
Figure 4.19 Derivative of the sliding surface of SMC based ABS with various initial speeds for nominal road . . . . .	51
Figure 4.20 Sliding surface of SMC based ABS with various initial speeds for slippery road . . . . .	51
Figure 4.21 Derivative of the sliding surface of SMC based ABS with various initial speeds for slippery road . . . . .	52

# Chapter 1

## Introduction

### 1.1 Background of the Study

In Automatic highway system, automatic brake actuation is a very important part of the overall vehicle control system. The precise application of brake torque is essential to maintaining proper vehicle spacing (on the order of a meter is maintained during routine merge and following maneuvers) and ride quality on an automatic highway. Due to the nonlinearities of the brake actuation system, a faster response, and robust braking control system is crucial. For emergency maneuver requirement, the precise application of brake torque is crucial for avoiding the wheel lock-up.

An Antilock Brake System (ABS) is system that modulates the brake torque that is applied to the wheel in order to prevent the controlled wheel from becoming fully locked. ABS is among the most important safety systems in a vehicle. It prevents the wheel lock-up under critical braking conditions, such as those encountered with dry or slippery road surfaces and driver panic reaction [1]. By preventing the wheel lock-up, ABS ensures that the vehicle remains responsive to steering wheel inputs. Reduced stopping distance on account of ABS is more evident on dry or slippery road surfaces [2].

### 1.2 Statements of the Problem

ABS is one of the automotive industry's most recent attempts in enhancing passenger safety specifically related to accident avoidance. However, designing an ABS is a challenging task considering the fact that it is highly nonlinear and a time varying system. The interaction between the tires and the road surface, the dynamics of the whole vehicle and the characteristics of key components in ABS (such as valves, brake chambers and brake pads) are all nonlinear and time varying. Although a linear model can be derived through simplification, it is less accurate thus impedes the use of some advanced control strategy. Due to the nonlinearities of the brake actuation system, a faster response, and robust braking control system with a faster

response is required to handle even sudden, extreme variations in driving conditions with little loss of traction and steering ability. The vehicle could stop optimally regardless of split surface condition while directional stability and control is maintained. For emergency maneuver requirement, the precise application of brake torque is crucial for avoiding the wheel lock-up. To resolve these difficulties various types of control mechanisms are applied [3][4] [5] [6] [7] . Out of these control mechanisms, sliding mode control design of antilock brake system is preferable than those from a locked wheel stop, because of the following advantages [8]:

- The dynamic behavior of the system may be tailored by the particular choice of sliding surface
- The order of the system dynamic under a sliding motion reduces by a number of inputs
- An n-dimensional tracking problem is converted to a lower order stabilization problem etc.

Generally, in this thesis we proposed and evaluate the control system based on the stopping distance, steerability and stability of a system.

### **1.3 Objectives of the thesis**

The main objective of this work is to design a sliding mode control for antilock braking system of a vehicle that attains vehicle stability, minimal stopping distance and steerability of a wheel.

The specific objectives are;

- \* To develop mathematical model for antilock braking system.
- \* To simulate the existing model in different road scenarios.
- \* To design sliding mode controller based antilock braking system.
- \* To evaluate the performance of the designed sliding mode controller using MATLAB.

### **1.4 Methodology**

Our study firstly undertakes study of literatures about controller designs and theoretical backgrounds about electromagnetic braking system and controller. After we have gotten a good understanding about antilock braking system and electromagnetic braking system from the literatures, we have compared various controller performances and then an appropriate technique is selected to improve the shortcomings of the system.

Since appropriate modelled dynamic equation of a vehicle has a vital role in controlling of a nonlinear system, the thesis has two modelling phases. Firstly, the dynamic models of the wheel and the vehicle are developed by using Newton's second law of motion. Then by integrating vehicle speed, wheel speed and some necessary assumptions, an appropriate system dynamics based on wheel slip is developed.

Secondly, to have a suitable realization of the system dynamic model for our controller design, the developed wheel and vehicle dynamic models are represented by using the nonlinear state space representation. During this representation, the wheel speed and vehicle speed are taken as state variables, and the torque applied to the wheel as the input variable.

After the dynamic models have been developed, the ABS controller is designed based on SMC theory. During controller design, a nonlinear sliding surface based on the variation of the desired and actual wheel slip is defined for handling the problem of chattering.

After the controller is designed, the stability of the system is investigated from the sliding surface by using Lyapunov stability method. The different vehicle parameters that are necessary for computer simulations are taken from Literatures.

The performance of the proposed method is examined through numerical simulations by using MATLAB. Moreover, the proposed controller is tested by using three different road types and three different vehicle speed scenarios that have a different initial speed.

## **1.5 Literature Review**

ABS is one of the automotive industry's most recent attempts in enhancing passenger safety specifically related to accident avoidance. However, designing an ABS is a challenging task considering the fact that it is highly nonlinear and a time varying system. Due to the nonlinearity property, some of control techniques have been implemented in the ABS system. Researchers have greatly improved the performance of ABS by utilizing different type of control algorithms such as sliding mode control and fuzzy logic control.

The well-known PID has been used to improve the performance of the ABS. Song, et al. [4] presented a mathematical model that is designed to analyze and improve the dynamic performance of a vehicle. A PID controller for rear wheel steering is designed to enhance the stability, steerability, and driveability of the vehicle during transient maneuvers. The PID controller is simple in design but there is a clear limitation of its performance. It does not possess enough robustness for practical implementation.

The model-based approach in Drakunov et al. [3] applies a search for the optimum brake

torque via sliding modes. This approach considers the friction force as an output, hence, a sliding observer is used to estimate it. This is not based on slip controller (the slip being not measurable). The approach is tested in a simplified simulation environment.

Recently, fuzzy logic controls (FLC) have been applied to ABS control problems [5] [6]. It employs a heuristic reasoning from human experiences and expert knowledge. FLC does not require an accurate mathematical model. Madau, et al. [9] presented a design of fuzzy logic ABS for a limited range coefficient of friction surface and tested it on an experimental brake system. Simulation results for the high  $\mu$  surface achieved were comparable to that of a production ABS controller. For the low  $\mu$  surface, the performance was found to be surprisingly functional. However, it was simulated with a minor tuning of the rules. Thus, the work required additional rules to handle various braking manoeuvre and road surface. Through the review of the ABS literature, it is clear that the implementation of ABS is focused on slip control. The concept of ABS has been described and shown that maintaining the wheel slip at the peak point of the  $\mu$ -slip curve is ideal to prevent the wheels from being totally locked during panic braking in order to achieve a shorter stopping distance and maintain a good steering ability.

## 1.6 Scope of the thesis

The scope of the thesis can be summarized in to three categories as follows:

1. A wheel slip based nonlinear state space representation of the system dynamic model is developed for the design of SMC based ABS of a vehicle. Under this we developed
  - Wheel dynamics, Vehicle dynamics and then develop the combined system which is written in state variable form considering the straight line braking with zero steering wheel input.
  - A nonlinear approach for controlling the ABS system based on Sliding Mode Controller (SMC)
2. We developed MATLAB code using different road scenario and initial velocity.
3. The performance of the designed SMC based ABS of the vehicle is investigated by using MATLAB. In addition to this, comparative study and performance analysis of the proposed control strategy is done.

## 1.7 Outline of the Thesis

This thesis is organized into five chapters. In Chapter 1 introductions and the problems observed on ABS of a vehicle are stated clearly. In addition to this the overall tasks, Literature reviews, scopes and the methods used for achieving the main objective are shortly summarized.

Chapter 2 gives a short definitions, types and principle of operations of ABS. Also describes about the derivation of nonlinear equations of motion for the vehicle and the wheel. In order to control the wheel slip, vehicle system dynamic equations are given in terms of wheel slip. And then, a suitable representation of the system dynamic model for the controller design is developed by using state space representation.

Chapter 3 a sliding mode controller based antilock braking system of a vehicle is designed. The objective of this brake control system is to keep the wheel slip at an ideal value under different road conditions so that the tire can still generate lateral and steering forces as well as shorter stopping distances. The system shows the nonlinearities and uncertainties (both uncertainty of the parameters and unmodeled system dynamics).

Hence, a nonlinear control strategy based on sliding mode is a standard approach to tackle the parametric and modelling uncertainties of a nonlinear system, it is chosen for slip control.

In Chapter 4 a nominal and SMC based ABS of a vehicle is simulated in MATLAB and their performance is evaluated under different road scenarios and various vehicle speeds.

Finally, chapter 5 summarizes the work done and results obtained. Recommendations for future work are also presented.

# Chapter 2

## Antilock Braking System

### 2.1 Introduction

This chapter provides an overview of an Antilock Braking System (its history and function), followed by a theoretical background of ABS control system. Modeling of ABS (wheel dynamics, vehicle dynamics, combined system) is clearly explained and also system dynamics in terms of wheel slip is also discussed.

### 2.2 Antilock Braking System

The current hydraulic ABS systems were conceived from systems developed for trains in the early 1900's. ABS was also developed to assist aircrafts to stop immediately and quickly on slippery runways. In 1947, Boeing Corporation developed the first ABS for airplanes [10]. It was too expensive for automotive at that time. The first automotive use of ABS was in 1954 on a limited number of Lincolns which were fitted with an ABS from a French aircraft [11]. In the late 60's, Ford, Chrysler, and Cadillac offered ABS on very few models. These very first systems used analogue computers and vacuum-actuated modulators [11]. However; it was commercially not successful at this stage [12]. The real growth of ABS was in the 1970s. In the late 70's, Mercedes and BMW introduced electronically-controlled ABS systems. By 1985, Mercedes, BMW and Audi introduced Bosch ABS systems while Ford introduced its first Teves system [11]. By the late-80's, ABS systems were offered on many high-priced luxury and sports cars. Today, braking systems on most passenger cars and many light-duty vehicles have become complex, computer controlled systems ABS incorporates a number of subsystems. In most ABS systems there will be a slip controller subsystem [11]. Note that not all ABS systems estimate and control the wheel slip explicitly, but work on speed and acceleration instead. The wheel slip controllers for each wheel are only active in critical situations. Thus, each controller is switched off and the brake is set to manual operation when the wheel is no longer in danger of being locked. On the other hand, the slip controller has to be switched on early enough

to prevent the wheel from locking. Thus, the corresponding switching logic is crucial for the functionality of the ABS. The basic control-philosophy for conventional ABS systems is a combination of slip control and wheel acceleration control [13] [14] [15] [12]. Wheel acceleration control uses the measured wheel angular velocities to control indirectly the slip by regulating the acceleration/deceleration of the wheels. The actuator used in ABS systems is typically a hydraulic solenoid valve which has three brake pressure modes:

- increase
- hold
- reduce

The controller is switched on when the deceleration of the wheel drops below a specified value for a given period of time. As long as the ABS is active, the switching between the different actuator modes (increase, hold or reduce) is controlled either using several slip and acceleration thresholds or by defining a switching surface using a weighted sum of slip and acceleration. By appropriately selecting these thresholds, the slip will oscillate around the 'critical slip'. Thus, the friction force between the tyre and the road surface will be closed to its maximum value and the braking distance is minimized. Slip control works satisfactorily for non-decreasing tyre force characteristics while wheel acceleration control tends to work better for tyre characteristics which have a pronounced maximum [11]. This is due to the fact that a larger wheel acceleration/deceleration can be obtained in the pronounced maximum case. ABS controllers have been shown to be highly adaptive since they can tolerate a considerable amount of uncertainty in the tyre force characteristics and the friction coefficient.

The configuration of an ABS is illustrated in Figure 2.1. Typically, an ABS consists of three major parts [16]:

- (a) electronic sensors
- (b) an Electronic Control Unit (ECU)
- (c) electrically controlled valves

Electronic sensors measure the wheel velocities and the brake pressure, the vehicle velocity and/or the vehicle acceleration. Electronic Control Unit (ECU) is usually a microprocessor-based system and the electrically controlled valves are used to control the pressure in brake cylinder or chambers. The function of an ABS is to prevent wheels from being totally locked during panic braking or braking on slippery road surface. The objective of an ABS is to achieve

the shorter stopping distance and to maintain a good steering stability during braking. When a lockup wheel is detected, ECU releases the brake pressure until the wheel lockup is avoided. Then ABS re-applies braking when the wheel velocity speeds up again.

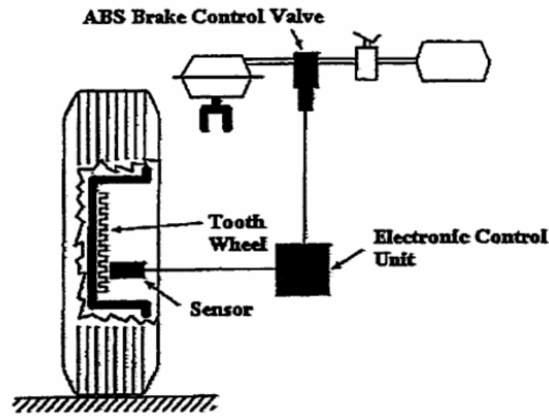


Figure 2.1: Configuration of an ABS [16]

There are two major torques acting on the wheel. The first is called the brake torque  $T_b$  that slows down the wheel velocity. The second is the torque from the road friction force or tyre force  $F_r$ . This torque actually accelerates the wheel velocity but slows down the vehicle velocity. Figure 2.2 illustrates the free body diagram of the wheel. At the beginning of braking, a vehicle and its wheels have initial velocities, which usually are the same under the normal driving conditions. During braking, the wheel velocity and the vehicle velocity are different.

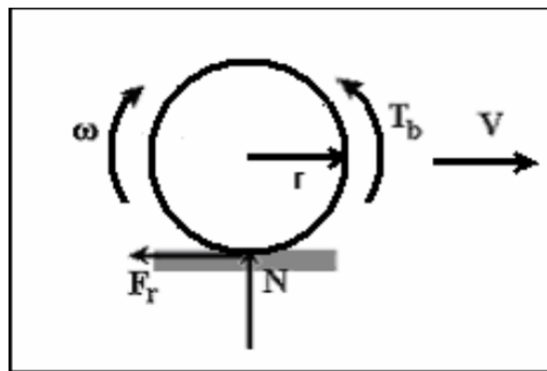


Figure 2.2: Free body diagram of single-wheel

The wheel velocity is always less than or equal to the vehicle velocity [16].

In (automotive) vehicle dynamics, slip is the relative motion between a tyre and the road surface it is moving on. This slip can be generated by the tyre's rotational speed being greater or less than the free-rolling speed. Mathematically the wheel slip ( $\lambda$ ) is defined as:

$$\lambda = \frac{v - \omega * r}{v} \quad (2.1)$$

Where  $v$  is the vehicle speed,  $\omega$  is the wheel speed and  $r$  is radius of wheel. From this equation, it can be explained that if the wheel velocity is zero ( $\omega = 0$ ), the wheel slip will equal to one ( $\lambda = 1$ ). It means that the wheel is locked. However, if  $v = \omega r$ , the wheel slip will equal to zero ( $\lambda = 0$ ). It is usually called free rolling.

The longitudinal coefficient ( $\mu$ ) of friction between tyre and road is a nonlinear function of the wheel slip ( $\lambda$ ). Figure 2.3 shows a typical curve illustrating the relation between  $\mu$  and  $\lambda$  for different road surface, which is called a  $\mu$ -slip curve. The longitudinal coefficient ( $\mu$ ) of friction equals zero at  $\lambda = 0$ . Typically, it exhibits a peak at some intermediate value of the wheel slip. For most surfaces,  $\mu$  increases with the wheel slip until a peak point is reached. Then it decreases as the wheel slip increases. Figure 2.3 also shows the lateral force which provides the lateral stability, i.e., the ability to steer a vehicle. As the wheel slip increase from  $\lambda = 0$  to  $\lambda = 1$ , the lateral force decreases from its maximum value to zero. If an excessive brake torque is applied, the wheel will be locked, which means that it slides on the road surface but does not rotate at all. A locked wheel has no lateral stability and less longitudinal friction force, which is the ultimate force to stop the vehicle. Thus, a braking with a locked wheel will cause longer stopping distance and lateral instability. Without ABS control, it is easy to analyze that in the increasing part of the  $\mu$ - slip curve in Figure 2.3, open loop braking is stable. But in the decreasing part of the  $\mu$ -slip curve, it is unstable. The tyre force from the road surface causes the wheel velocity to increase, thus decreases the wheel slip.

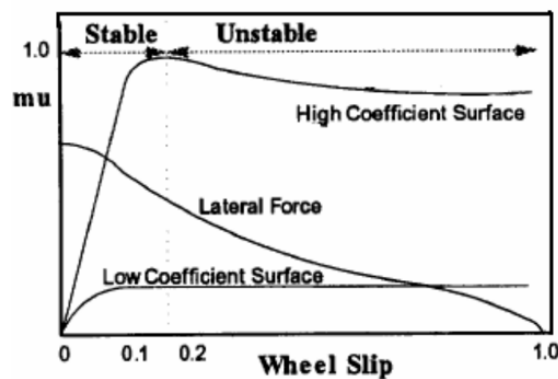


Figure 2.3: The  $\mu$ -slip curve [9]

A high  $\mu$  leads to a large tyre force and a low  $\mu$  leads to a small tyre force. In the increasing part of the  $\mu$ -slip curve, an increase of the wheel slip leads to a larger  $\mu$  and a larger tyre force, which reverses the wheel slip to a small value. However, in the decreasing part of the  $\mu$ -slip curve, an increase of the wheel slip leads to a smaller  $\mu$  and a smaller tyre force, which causes the wheel slip to increase continuously. So, the peak point of the  $\mu$ -slip curve is critical. When a braking is initiated, the wheel velocity starts to decrease and the wheel slip starts to increase from zero.

The wheel slip may stop increasing and start to decrease before the  $\mu$  reaches its peak point. But if an excessive brake torque is applied, the wheel slip may go straightly to a large number, which causes the  $\mu$  to pass its peak point and reach somewhere in the decreasing part of the  $\mu$ -slip curve. If the brake torque is not reduced quickly at this point, the reduction of the road friction force will lead to a rapid increase of the wheel slip and eventually to a wheel lockup. ABS tries to detect when this peak point is going to be reached and then reduces the brake torque properly so that a wheel lockup could be avoided. It appears to be true that maintaining the wheel slip at the peak point of the  $\mu$ - slip curve is ideal. As it is shown in Figure 2.4, the position of the peak  $\mu$  point varies on the different road surfaces. It can be seen in Figure 2.4. In addition, stay at the peak point of the  $\mu$ - slip curve sometime may lead to a poor lateral stability. Thus, many control strategies define their performance goal as maintaining the wheel slip near a value of 0.2 [16]. This represents a compromise between the lateral stability, which is best at  $\mu = 0$  and the maximum deceleration which usually appears when  $\lambda$  is between 0.1 and 0.3.

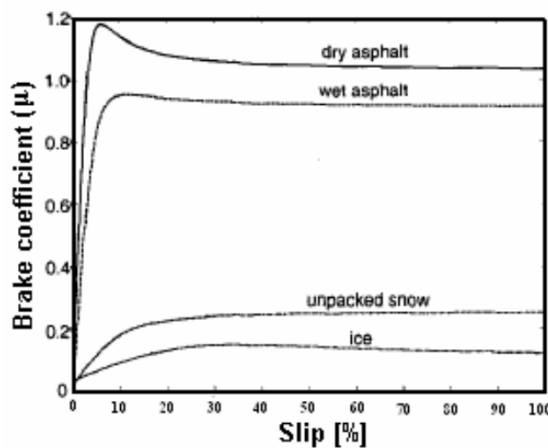


Figure 2.4: The  $\mu$ -slip curve varies on different road surface [1]

## 2.3 Modeling of Antilock Braking System

In order to design a controller, a good representative model of the system is needed. A vehicle mathematical model, which is appropriate for modeling both acceleration and deceleration, is described in this section. This model will be used for design of control laws and computer simulations. Although the model considered here is relatively simple, it retains the essential dynamics of the system. The model identifies the wheel speed and vehicle speed as state variables, and it identifies the torque applied to the wheel as the input variable. The two state variables in this model are associated with one-wheel rotational dynamics and linear vehicle dynamics. The state equations are the result of the application of Newton's law to wheel and

vehicle dynamics. The wheel and vehicle dynamic models are developed by using the following assumptions:

- The vehicle body does not undergo any change in size or shape (mass of the vehicle is constant).
- Wheel viscous friction can be taken as an external disturbance on the vehicle.
- Straight line braking with zero steering wheel input is considered.
- The engine dynamics is not considered.
- Constant engine torque is considered.

## Wheel (Rotational Motion ) Dynamics

As it is shown in Figure 3.1, the overall torques and forces that will act on the wheel of a vehicle are due to the influence of engine torque, brake torque, tire tractive force, wheel friction force, normal reaction force from the ground and gravitational force.

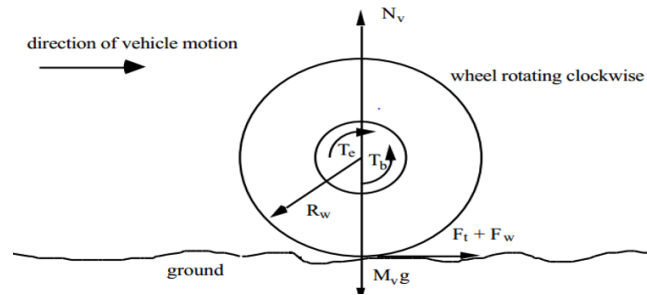


Figure 2.5: Wheel Dynamics

From Newton's law of motion the dynamic equation for the angular motion of the wheel is:

$$\begin{aligned} T_w &= J_w \alpha_w \\ &= T_e - T_b - R_w F_t - R_w F_w \end{aligned}$$

and we know that

$$\alpha_w = \dot{\omega}_w \quad (2.2)$$

then

$$\dot{\omega}_w = \frac{T_e - T_b - R_w F_t - R_w F_w}{J_w} \quad (2.3)$$

Where

The total torque acting on the wheel divided by the moment of inertia of the wheel equals the wheel angular acceleration (deceleration). The total torque consists of shaft torque from the engine, which is opposed by the brake torque and the torque components due to the tire

- $T_w$  = Torque of the wheel,  
 $J_w$  = the moment of inertia of the wheel,  
 $\alpha_w$  =angular acceleration of the wheel,  
 $\omega_w$  = the angular velocity of the wheel, the over dot indicates differentiation with respect to time,  
 $R_w$  =Radius of the wheel,  
 $N_v$  =Normal reaction force from the ground,  
 $T_e$  =Shaft torque from the engine,  
 $T_b$  =Brake torque,  
 $F_t$  =Tractive force and  
 $F_w$  =Wheel viscous friction.

tractive force and the wheel viscous friction force. The linear acceleration of the vehicle is equal to the difference between the total tractive force available at the tyre-road contact and the aerodynamic drag on the vehicle, divided by the mass of the vehicle. The tractive force is the average friction force of the driving wheels for acceleration and the average friction force of all wheels for deceleration. The total tractive force is equal to the product of the average friction force,  $F_t$ , and the number of wheels,  $N_w$ . The model of the tractive force is crucial [3]. This force depends on the road surface, tyre, weather, and many other conditions. The Pacejka model [17] has been used in many studies. In this model it is assumed that the tractive force at each wheel during braking is a nonlinear function of the relative slip  $\lambda$ . The tire tractive (braking) force is given by:

$$F_t = \mu(\lambda)N_v \quad (2.4)$$

Where the normal tire force (the reaction force from the ground to the tire),  $N_v$ , depends on vehicle parameters such as the mass of the vehicle, location of the center of gravity of the vehicle, and the steering and suspension dynamics. The normal load is described by standard Newtonian equation of motion given by:

$$N_v = m_t g + F_L \quad (2.5)$$

where  $m_t$  is the mass of quarter vehicle. The longitudinal weight transfer load due to braking,  $F_L$  is expressed by:

$$F_L = \frac{m_v h_{cg}}{2L} \dot{V} \quad (2.6)$$

Where

Applying a driving torque or a braking torque to a pneumatic tire produces tractive (braking) force at the tire-ground contact patch. The driving torque produces compression at the tire

- $m_v$  = mass of the vehicle,
- $h_{cg}$  = center of gravity height and
- $L$  = wheel base (the distance between the front and rear wheel)
- $V$  =Speed of the vehicle

tread in front of and within the contact patch. Consequently, the tire travels a shorter distance than it would if it were free rolling. In the same way, when a braking torque is applied, it produces tension at the tire tread within the contact patch and at the front. Because of this tension, the tire travels a larger distance than it would if it were free rolling. This phenomenon is referred as the wheel slip or deformation slips[18][19]. The adhesion coefficient, which is the ratio between the tractive (braking) force and the normal load, depends on the road-tire conditions and the value of the wheel slip  $\lambda$  [20]. Figure 3.2. shows a typical  $\mu(\lambda)$  curve. Mathematically, wheel slip is defined as:

$$\lambda = \frac{\omega_w - \omega_v}{\omega}, \omega \neq 0 \quad (2.7)$$

Where

$$\omega_v = \frac{V}{R_w}$$

The variable  $\omega$  is defined as:

$$\omega = \max(\omega_w, \omega_v) \quad (2.8)$$

This is the maximum vehicle angular velocity and wheel angular velocity. The adhesion coefficient  $\mu(\lambda)$  is a function of wheel slip  $\lambda$ . For various road conditions, the  $\mu(\lambda)$  curves have different peak values and slopes, as shown in Figure 3.3. The function  $\mu(\lambda) = \frac{2\lambda\mu_p\lambda_p}{\lambda_p^2 + \lambda^2}$  is used for a nominal curve, where  $\mu_p$  and  $\lambda_p$  are the peak values. As shown in Figure 3.2, For various road conditions, the curves have different peak values and slopes. The adhesion coefficient slip characteristics are also influenced by operational parameters such as speed and vertical load. The peak value for the adhesion coefficient usually has values between 0.1 (icy road) and 0.9 (dry asphalt and concrete).

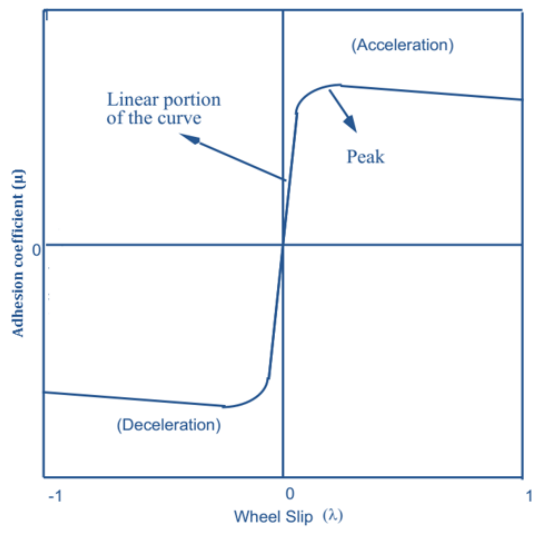


Figure 2.6: Typical  $\mu - \lambda$  characteristics curve[20].

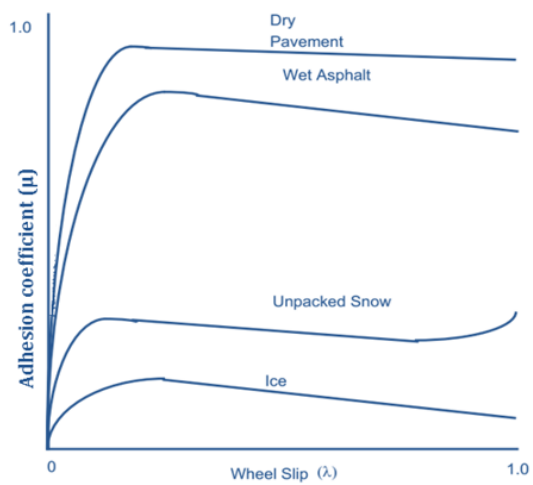


Figure 2.7: Curves for Different Road conditions [20].

## Vehicle Dynamics

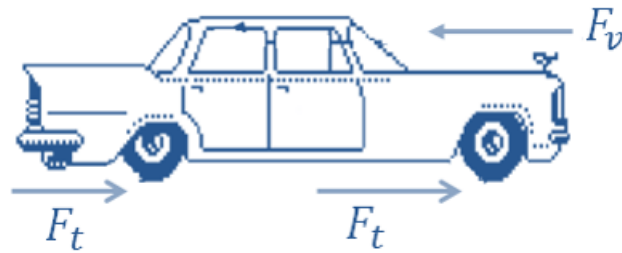


Figure 2.8: Vehicle dynamics

As it is shown in Figure 3.4, the dynamic model of the vehicle can be derived from Newton's law of motion as the following:

$$F = ma \quad (2.9)$$

where:  $a = \frac{dV}{dt}$  then

$$F = \frac{m dV}{dt} = m\dot{V} \quad (2.10)$$

But from the Figure 3.4

$$F = N_w F_t - F_v = m_v \dot{V} \quad (2.11)$$

Therefore; the dynamic equation for the vehicle motion is:

$$\dot{V} = \frac{N_w F_t - F_v}{m_v} \quad (2.12)$$

Where:

$F_v$  = wind drag force (function of vehicle velocity),

$a$  = acceleration,

$m_v$  = vehicle mass

$N_w$  = number of driving wheels (during acceleration) or the total number of wheels (during braking), and

$F_t$  = tire tractive force,

The linear acceleration of the vehicle is equal to the difference between the total tractive force available at the tire-road contact and the aerodynamic drag on the vehicle, divided by the mass of the vehicle. The total tractive force is equal to the product of the average friction force,  $F_t$ , and the number of wheels,  $N_w$ .

Drag is largest and most important aerodynamic force encountered by passenger cars at normal highway speed [21]. The overall drag on a vehicle is derived from contributions of many sources. The aerodynamic drag is a nonlinear function of the vehicle velocity and is highly dependent on weather conditions [22]. The drag from air resistance depends on the dynamic pressure, and is thus proportional to the square of the speed. The equation of aerodynamic drag force for the quarter car vehicle model is given by

$$F_v = \frac{1}{4} \left( \frac{\rho}{2} C_d A_f V^2 \right) \quad (2.13)$$

Where:

- $F_v$  = aerodynamic drag force,
- $\rho$  = air density,
- $C_d$  = aerodynamic drag coefficient,
- $A_f$  = frontal area of the vehicle,
- $V$  = vehicle speed

Frontal area of the vehicle can be obtained by:

$$A_f = w * h * 85\%$$

and wheel viscous friction

$$F_w = c * m * g$$

where:

- $c$  = Coefficient of friction of the surface.
- $w$  = is the width of the vehicle.
- $h$  = is height of the vehicle.

### 2.3.1 Combined System

The dynamic equation of the whole system can be written in state space representation form by defining convenient state variables. Using Equations (3.2) and (3.11), the state variables are

defined as the following:

$$x_1 = \frac{v}{R_w} \quad (2.14)$$

$$x_2 = \omega_w \quad (2.15)$$

Differentiating the above two equations with respect to time and equating it with the respective Equations of 3.2 and 3.11 will results the following.

$$\dot{x}_1 = -f_1(x_1) + b_1\mu(\lambda) \quad (2.16)$$

$$\dot{x}_2 = -f_2(x_2) - b_2\mu(\lambda) + b_3 T \quad (2.17)$$

where:

$$\begin{aligned} T &= T_e - T_b \\ f_1(x_1) &= \frac{F_v}{M_v R_w} \\ b_1 &= \frac{N_v N_w}{M_v R_w} \\ f_2(x_2) &= \frac{F_w(x_2)}{J_w} \\ b_2 &= \frac{R_w N_V}{J_w} \\ b_3 &= \frac{1}{J_w} \end{aligned} \quad (2.18)$$

The combined dynamic system can be represented as shown in Figure 3.5. The control input is the applied torque at the wheels, which is equal to the difference between the shaft torque from the engine and the braking torque. During acceleration, engine torque is the primary input while during deceleration; the braking torque is the primary input.

### 2.3.2 System Dynamics In Terms of Wheel Slip

Wheel slip is chosen as the controlled variable for braking control algorithms because of its strong influence on the braking force between the tire and the road. By controlling the wheel slip, we can manage the braking force to obtain the desired output of the system. In order to have an ease model for the controller design, the system dynamic model can be formulated in-terms of wheel slip. During deceleration the angular velocity of the wheel is less than to as that of the angular velocity of the vehicle. Then Equations 3.6 and 3.7 can be expressed by using state variables as the following.:

$$\lambda = \frac{x_2 - x_1}{x_1} \quad (2.19)$$

By differentiating the above equation with respect to time and substituting  $x_2 = x_1(1 + \lambda)$  in to the differentiated equation, we will obtain the following.

$$\dot{\lambda} = \frac{\dot{x}_2 - (1 + \lambda)\dot{x}_1}{x_1} \quad (2.20)$$

Substituting Equations (3.15) (3.16) and (3.18) into Equation (3.19), will yields the following.

$$\dot{\lambda} = \frac{[(1 + \lambda)f_1(x_1) - f_2(x_2)] - [b_2 + (1 + \lambda)b_1]\mu + b_3 T}{x_1} \quad (2.21)$$

Equation 3.20 represents the wheel slip based dynamic model of the system for a decelerating vehicle. Where as if the vehicle is accelerating, Equation 3.20 will be modified in to the following equation.

$$\dot{\lambda} = \frac{[f_1(x_1) - (1 - \lambda)f_2(x_2)] - [b_1 + (1 - \lambda)b_2]\mu + b_3 T}{x_2} \quad (2.22)$$

This equation is nonlinear and involves uncertainties in its parameters. The nonlinear characteristics of the equation are due to the following:

- \* The relationship of wheel slip with velocity is nonlinear,
- \* The  $\mu - \lambda$  relationship is nonlinear,
- \* There are multiplicative terms in the equation,
- \* Functions  $f_1(x_1)$  and  $f_2(x_2)$  are nonlinear

The uncertainties of the parameters are due to the following:

- \* Normal tire force( $N_v$ ) changes based on steering and suspension dynamics
- \* The  $\mu - \lambda$  curve changes based on road surface
- \* Moment of inertia of the wheel is changing all the time
- \* Wind drags force changes based on uncertain wind speed and direction

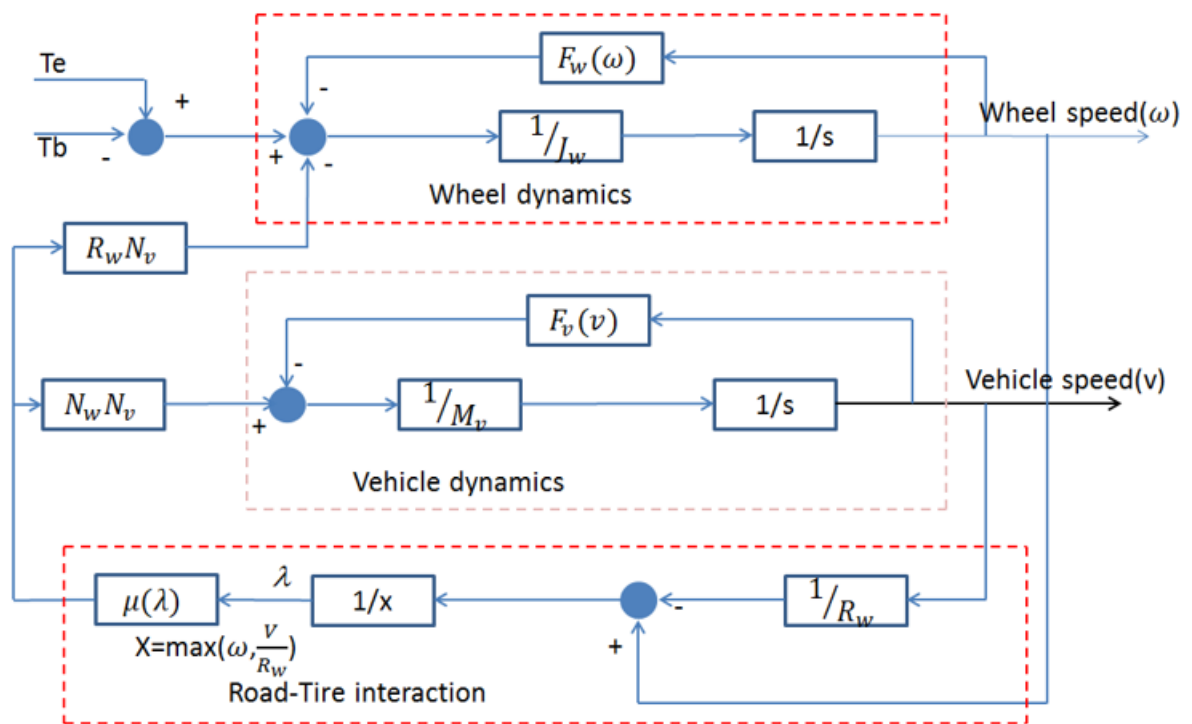


Figure 2.9: Vehicle/road/tire one-wheel model

# Chapter 3

## Design of Sliding Mode Controller Based Antilock Braking System

### 3.1 Introduction

In this chapter, a controller is designed for the ABS of a vehicle in order to achieve the desired wheel slip of the system. Control of braking force is attained by controlling the wheel slip because of the relationship between wheel slip and adhesion coefficient that is caused by road-tire interaction. As it is shown in chapter 3, the developed dynamic model is nonlinear and it has uncertainties on the system. . Hence, in order to tackle the parametric and modeling uncertainties of a nonlinear system, a nonlinear control strategy based on sliding mode is chosen for slip control.

### 3.2 Sliding Mode Control

SMC is one of the popular strategies to deal with uncertain control systems [23]. The main feature of SMC is the robustness against parameter variations and external disturbances and it is widely used to obtain good dynamic performance of control systems. Various applications of SMC have been conducted, such as vehicle, robotic manipulators, aircrafts, DC motors, chaotic systems etc. [22][24] [25]. Nonlinear system model imprecision may come from actual uncertainty about the plant (e.g., unknown plant parameters), or from the purposeful choice of a simplified representation of the system's dynamics. Modeling inaccuracies can be classified into two major kinds: structured (or parametric) uncertainties and unstructured uncertainties (or unmodeled dynamics). The first kind corresponds to inaccuracies on the terms actually included in the model, while the second kind corresponds to inaccuracies on the system order. Modeling inaccuracies can have strong adverse effects on nonlinear control systems. One of the most important approaches to dealing with model uncertainty is robust control. The typical structure of a robust controller is composed of a nominal part, similar to a feedback control

law, and additional terms aimed at dealing with model uncertainty. Sliding mode control is an important robust control approach. For the class of systems to which it applies, sliding mode controller design provides a systematic approach to the problem of maintaining stability and consistent performance in the face of modeling imprecision. On the other hand, by allowing the tradeoffs between modeling and performance to be quantified in a simple fashion, it can illuminate the whole design process.

### 3.2.1 Sliding Surfaces

This section investigates VSC as a high-speed switched feedback control resulting in sliding mode. For example, the gains in each feedback path switch between two values according to a rule that depends on the value of the state at each instant. The purpose of the switching control law is to drive the nonlinear plant's state trajectory onto a pre-specified (user-chosen) surface in the state space and to maintain the plant's state trajectory on this surface for subsequent time. The surface is called a switching surface. When the plant state trajectory is "above" the surface, a feedback path has one gain and a different gain if the trajectory drops "below" the surface. This surface defines the rule for proper switching. This surface is also called a sliding surface (sliding manifold). Ideally, once intercepted, the switched control maintains the plant's state trajectory on the surface for all subsequent time and the plant's state trajectory slides along this surface.

The most important task is to design a switched control that will drive the plant state to the switching surface and maintain it on the surface upon interception. A Lyapunov approach is used to characterize this task.

Lyapunov method is usually used to determine the stability properties of an equilibrium point without solving the state equation. Let  $V(\lambda)$  be a continuously differentiable scalar function defined in a domain  $D$  that contains the origin. A function  $V(\lambda)$  is said to be positive definite if  $V(0) = 0$  and  $V(\lambda) < 0$  for  $\lambda$ . It is said to be negative definite if  $V(0) = 0$  and  $V(\lambda) > 0$  for  $\lambda$ . Lyapunov method is to assure that the function is positive definite when it is negative and function is negative definite if it is positive. In that way the stability is assured.

A generalized Lyapunov function, that characterizes the motion of the state trajectory to the sliding surface, is defined in terms of the surface. For each chosen switched control structure, one chooses the "gains" so that the derivative of this Lyapunov function is negative definite, thus guaranteeing motion of the state trajectory to the surface. After proper design of the surface, a switched controller is constructed so that the tangent vectors of the state trajectory point towards the surface such that the state is driven to and maintained on the sliding surface. Such

controllers result in discontinuous closed-loop systems.

Let a single input nonlinear system be defined as

$$\lambda^{(n)} = f(\lambda, t) + b(\lambda, t)u(t) \quad (3.1)$$

Here,  $\lambda(t)$  is the state vector,  $u(t)$  is the control input (in this case braking torque or pressure on the pedal) and  $\lambda$  is the output state of the interest (in this case, wheel slip). The other states in the state vector are the higher order derivatives of  $\lambda$  up to the  $(n-1)^{th}$  order. The superscript  $n$  on  $\lambda(t)$  shows the order of differentiation.  $f(\lambda, t)$  and  $b(\lambda, t)$  are generally nonlinear functions of time and states. The function  $f(\lambda)$  is not exactly known, but the extent of the imprecision on  $f(\lambda)$  is upper bounded by a known, continuous function of  $\lambda$ ; similarly, the control gain  $b(\lambda)$  is not exactly known, but is of known sign and is bounded by known, continuous functions of  $\lambda$ . The control problem is to get the state  $\lambda$  to track a specific time-varying state  $\lambda_d$  in the presence of model imprecision on  $f(\lambda)$  and  $b(\lambda)$ . A time varying surface  $S(t)$  is defined in the state space  $R^{(n)}$  by equating the variable  $S(\lambda; t)$ , defined below, to zero.

$$S(\lambda; t) = \frac{1}{k} \lambda_e(t) + \int_0^t \lambda_e(\tau) d\tau \quad (3.2)$$

Here,  $k(\lambda, t)$  is the gain of the linear term on the sliding surface which is a strict positive constant, taken to be the bandwidth of the system, and  $\lambda_e(t) = \lambda(t) - \lambda_d(t)$  is the error in the output state where  $\lambda_d(t)$  is the desired state. The problem of tracking the  $n$ -dimensional vector  $\lambda_d(t)$  can be replaced by a first-order stabilization problem in  $S$ .  $S(\lambda; t)$  verifying (4.2) is referred to as a sliding surface, and the system's behavior once on the surface is called sliding mode or sliding regime. From Equation (4.2) the expression of  $S$  contains  $\int_0^t \lambda_e(\tau)$ . we only need to differentiate  $S$  once for the input  $u$  to appear. Furthermore, bounds on  $S$  can be directly translated into bounds on the tracking error vector  $\lambda_e$ , and therefore the scalar  $S$  represents a true measure of tracking performance. The corresponding transformations of performance measures assuming  $\lambda_e(0) = 0$  is:

$$\forall t \geq 0, |S(t)| \leq \phi \Rightarrow \forall t \geq 0, |\lambda_e^{(i)}(t)| \leq (2k)^i \epsilon \text{ For } i = 0, \dots, n-1 \quad (3.3)$$

Where  $\epsilon = \frac{\phi}{k^{n-1}}$  [8]. In this way, an  $n^{th}$ -order tracking problem can be replaced by a  $1^{st}$ -order stabilization problem. The simplified,  $1^{st}$ -order problem of keeping the scalar  $S$  at zero can now be achieved by trajectories choosing the control law  $u$  of Equation (4.1) such that outside of  $S(t)$ .

$$\frac{1}{2} \frac{d}{dt} S^2 \leq -\eta |S| \quad (3.4)$$

Where  $\eta$  is strictly positive constant. The condition that is described as Equation (4.4) states that the squared "distance" to the surface, as measured by  $S^2$ , decreases along all system trajec-

tories. Thus, it constrains to point towards the surface  $S(t)$ . In particular, once on the surface, the system trajectories remain on the surface. In other words, satisfying the sliding condition makes the surface an invariant set (a set for which any trajectory starting from an initial condition within the set remains in the set for all future and past times). Furthermore Equation (4.4) also implies that some disturbances or dynamic uncertainties can be tolerated while still keeping the surface an invariant set. Finally, satisfying Equation (4.2) guarantees that if  $\lambda(t = 0)$

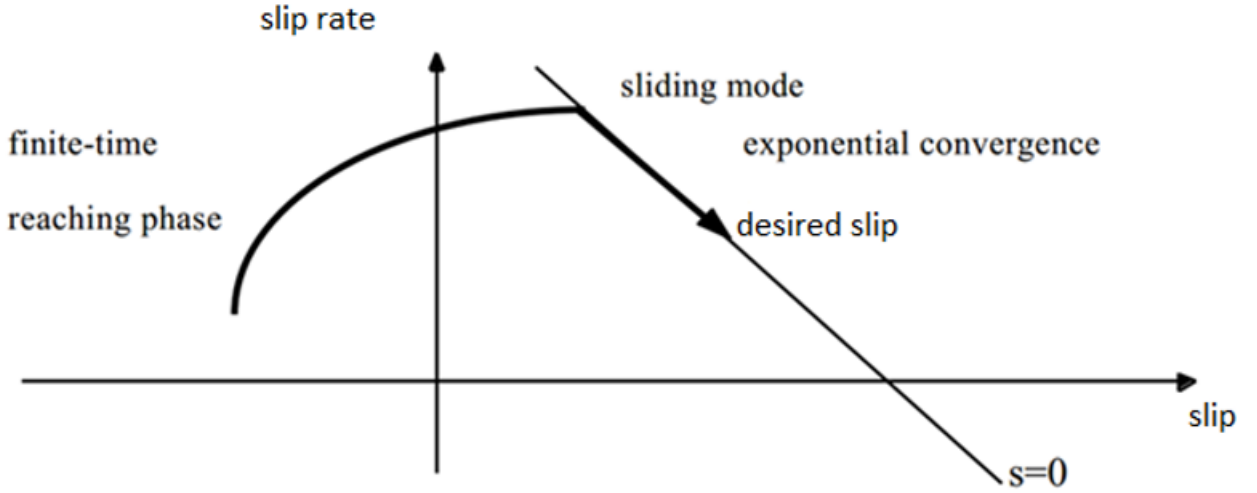


Figure 3.1: Graphical interpretation of Equations (4.2) and (4.4) ( $n=2$ ) [23]

is actually off  $\lambda_e(t = 0)$ , the surface  $S(t)$  will be reached in a finite time smaller than  $s(t = 0)/\eta$ . Assume for instance that  $s(t = 0) > 0$ , and let  $t_{reach}$  be the time required to hit the surface  $s = 0$ . Integrating Equation (4.4) between  $t = 0$  and  $t_{reach}$  leads to

$$0 - S(t = 0) = S(t = t_{reach}) - S(t = 0) \leq -\eta(t_{reach} - 0)$$

This implies that

$$t_{reach} \leq S(t = 0)/\eta$$

The similar result starting with  $S(t = 0) > 0$  can be obtained as

$$t_{reach} \leq |S(t = 0)|/\eta$$

Starting from any initial condition, the state trajectory reaches the time-varying surface in a finite time smaller than  $|S(t = 0)|/\eta$ , and then slides along the surface towards  $\lambda_d(t)$  exponentially, with a time-constant equal to  $\frac{1}{\lambda}$ . In summary, the idea is to use a well-behaved function of the tracking error,  $S$ , according to Equation (4.2), and then selecting the feedback control law  $u$  in Equation (4.1) such that  $S^2$  remains characteristic of a closed-loop system, despite the presence of model imprecision and of disturbances.

## Chattering

Chattering is a phenomenon of high frequency switching of the control action which causes high frequency oscillations in the output, heating up of electrical circuits and premature wear in actuators. Basically, the high frequency components of the control propagate through the system, therefore, exciting the unmodeled fast dynamics, and undesired oscillations affect the system output. This can degrade the system performance or may even lead to instability. Chattering has been also designated to indicate the bad effect potentially disruptive that a switching control force (torque) can produce on a control mechanical plant [26]. An ideal sliding mode exists only when the state trajectory  $x(t)$  of the controlled plant agrees with the desired trajectory at every  $t_1$  for some  $t_1$ . This may require infinitely fast switching. In real systems, a switched controller has imperfections which limit switching to a finite frequency. The representative point then oscillates within a neighborhood of the switching surface. Control laws which satisfying sliding condition (4.4) and lead to "perfect" tracking in the face of model uncertainty, are discontinuous across the surface  $S(t)$ , thus causing control chattering. Chattering is undesirable, since it involves extremely high control activity, and furthermore may excite high-frequency dynamics neglected in the course of modeling. Chattering must be reduced (eliminated) for the controller to perform properly. This can be achieved by smoothing out the control discontinuity in a thin boundary layer neighboring the switching surface

$$B(t) = \{\lambda, |\lambda; t| \leq \phi\} \quad \phi > 0 \quad (3.5)$$

Where  $\phi$  is the boundary layer thickness, and  $\epsilon = \frac{\phi}{k^{n-1}}$  is the boundary layer width. In other words, outside of  $B(t)$ , we choose control law as before which guarantees that the boundary layer is attractive, hence invariant; all trajectories starting inside  $B(t = 0)$  remain inside  $B(t)$  for all  $t \geq 0$ ; and then  $u$  is interpolated inside  $B(t)$ . For example,  $sgn(s)$  in (4.12) can be replaced by  $\frac{s}{\phi}$  inside  $B(t)$ .

This approach leads to tracking to within a guaranteed precision (rather than perfect tracking), and more generally guarantees that for all trajectories starting inside  $B(t = 0)$

$$\forall t \geq 0, |\lambda^i| \leq (2k)^i \epsilon \quad i = 0 \cdots n-1 \quad (3.6)$$

### 3.2.2 Controller Design

The controller design procedure consists of two steps. First, a feedback control law  $u$  is selected to verify sliding condition that is described as Equation (4.4). However, in order to account for

the presence of modeling imprecision and of disturbances, the control law has to be discontinuous across  $S(t)$ . As it is shown in appendix C, Since the implementation of the associated control switching is imperfect, this leads to chattering. chattering is undesirable in practice, since it involves high control activity and may excite high frequency dynamics neglected in the course of modeling. Thus, in a second step, the discontinuous control law  $u$  is suitably smoothed to achieve an optimal trade-off between control bandwidth and tracking precision. The first step achieves robustness for parametric uncertainty; the second step achieves robustness to high frequency unmodeled dynamics. This section discusses the first step. Then we know that our system is:

$$\dot{\lambda}(t) = f(\lambda, t) + b(\lambda, t)u(t) \quad (3.7)$$

Where:  $f(\lambda, t) = \frac{((1+\lambda)f_1(x_1) - f_2(x_2) - [b_2 + (1+\lambda)b_1]\mu(\lambda))}{x_1}$  is generally nonlinear and/or time varying and is estimated as  $\hat{f}(\lambda, t)$ ,  $u(t) = T$  is the control input,  $\lambda(t) =$  is the state to be controlled so that it follows a desired trajectory  $\lambda_d(t)$  and  $b(\lambda, t) = \frac{b_3}{x_1}$ . The estimation error on  $f(\lambda, t)$  is assumed to be bounded by some known function  $F = F(\lambda, t)$ , so that

$$|\hat{f}(\lambda, t) - f(\lambda, t)| \leq F(\lambda, t)^1 \quad (3.8)$$

As it is already expressed in Equation (4.2), the defined sliding surface is:

$$S(\lambda; t) = \frac{1}{k} \lambda_e(t) + \int_0^t \lambda_e(\tau) d(\tau) \quad (3.9)$$

In order to find control to reach  $S(\lambda, t)$  and stay there after, the control input can be partitioned in to two parts:

$$U(t) = u_c(t) + u_{eq}(t) \quad (3.10)$$

Where the corrective control  $u_c(t)$  is used to compensate the deviations from the sliding surface to reach the sliding surface; whereas the equivalent control  $u_{eq}(t)$  is used to make the derivative of the sliding surface equal to zero to stay on the sliding surface.

The control that drives the state to the sliding mode in a finite time can be obtained from the existence of the sliding mode. The sliding mode can exist if the derivative of the sliding surface equals to zero. By differentiating Equation 4.7 and equal to zero, we can obtain the equivalent control for our system.

$$\Rightarrow \dot{s}(\lambda, t) = 0$$

---

<sup>1</sup>See appendix A for the derivation of  $F(\lambda, t)$  for this particular application[23].

$$\begin{aligned}
&\Rightarrow \frac{1}{k} \dot{\lambda}_e + \frac{d}{dt} \left( \int_0^t \lambda_e d\tau \right) = 0 \\
&\Rightarrow \frac{1}{k} \frac{d}{dt} (\lambda - \lambda_d) + \lambda_e = 0 \\
&\Rightarrow \frac{1}{k} \dot{\lambda} + \lambda_e = 0
\end{aligned} \tag{3.11}$$

Substituting Equation (3.19) in to Equation (4.9) will yields the following:

$$\Rightarrow \frac{1}{k} \left\{ \frac{\dot{x}_2 - (1 + \lambda)x_1}{x_1} \right\} + (\lambda - \lambda_d) = 0 \tag{3.12}$$

Substituting Equation (3.15) and (3.16) into Equation (4.10) yields the equivalent control as shown below:

$$\begin{aligned}
&\Rightarrow \frac{1}{k} \left\{ \frac{-f_2(x_2) - b_2\mu(\lambda) + b_3U - (1 + \lambda)(-f_1(x_1) + b_1\mu(\lambda))}{X_1} \right\} + (\lambda - \lambda_d) = 0 \\
&\Rightarrow \left\{ \frac{-f_2(x_2) - b_2\mu(\lambda) + b_3U - (1 + \lambda)(-f_1(x_1) + b_1\mu(\lambda)) + kx_1(\lambda - \lambda_d)}{kx_1} \right\} = 0 \\
&\Rightarrow (-f_2(x_2) - b_2\mu(\lambda) + b_3U - (1 + \lambda)(-f_1(x_1) + b_1\mu(\lambda)) + kx_1(\lambda - \lambda_d)) = 0 \\
&\Rightarrow b_3U = f_2(x_2) + b_2\mu(\lambda) + (1 + \lambda)(-f_1(x_1) + b_1\mu(\lambda)) - kx_1(\lambda - \lambda_d) \\
&\Rightarrow U_{eq} = \frac{f_2(x_2) + b_2\mu(\lambda) + (1 + \lambda)(-f_1(x_1) + b_1\mu(\lambda)) - kx_1(\lambda - \lambda_d)}{b_3}
\end{aligned} \tag{3.13}$$

$u_{eq}(t)$  Can interpret as the best estimate of the equivalent control. Since the corrective control law is used to compensate the deviations from the sliding surface to reach the sliding surface, for our system it can be defined as the following.

$$u_c(t) = -X_1 \text{sign}(s(t)) \tag{3.14}$$

In general, the overall automatic control law for this braking system is:

$$\Rightarrow U(t) = u_{eq}(t) - X_1 \text{sign}(s(t)) \tag{3.15}$$

$$\Rightarrow U(t) = \frac{1}{b_3} \{f_2(x_2) + b_2\mu(\lambda) + (1 + \lambda)(-f_1(x_1) + b_1\mu(\lambda)) - kx_1(\lambda - \lambda_d)\} - X_1 \text{sign}(s) \tag{3.16}$$

Referring to Lyapunov stability method [27], the system in Equation (4.5) is asymptotically stable to  $S(\lambda; t) = 0$  for the entire initial condition  $\lambda(t_0) \in \Omega$ , where  $\Omega = \{\lambda : \dot{V}(\lambda, t) < 0, \forall t\}$ , if  $\dot{V}(\lambda, t) < 0$  evaluated along a solution  $\lambda$  for all  $\lambda \in \Omega$ . To prove convergence to the sliding mode, we want to show that with this control  $U(t)$ ,  $S$  should converge to 0 in finite time. Consider that, the Lyapunov function for evaluating the stability of the system is

$$V = \frac{1}{2}S^2 \quad (3.17)$$

The system that is described in Equation (4.5) is stable if and only if the derivative of the Lyapunov function is negative.

$$\Rightarrow \dot{V} < 0$$

$$\Rightarrow S\dot{S} < 0$$

$$\Rightarrow S \left\{ \frac{1}{k} \dot{\lambda}_e + \frac{d}{dt} \left( \int_0^t \lambda_e d\tau \right) \right\} < 0 \quad (3.18)$$

$$\Rightarrow S \left\{ \frac{1}{k} \dot{\lambda} + \lambda_e \right\} < 0 \quad (3.19)$$

$$\Rightarrow s \left\{ \frac{1}{k} \left\{ \frac{\dot{x}_2 - (1 + \lambda)x_1}{x_1} \right\} + (\lambda - \lambda_d) \right\} < 0 \quad (3.20)$$

substituting Equation(3.15) and (3.16) in to Equation (4.18), yields:

$$\Rightarrow S \left\{ \frac{1}{k} \left\{ \frac{-f_2(x_2) - b_2\mu(\lambda) + b_3U - (1 + \lambda)(-f_1(x_1) + b_1\mu(\lambda))}{X_1} \right\} + (\lambda - \lambda_d) \right\} < 0 \quad (3.21)$$

$$\Rightarrow S \left\{ \left\{ \frac{(-f_2(X_2) - b_2\mu(\lambda) + b_3U) - (1 + \lambda)(-f_1(X_1) + b_1\mu(\lambda)) + kX_1(\lambda - \lambda_d)}{kX_1} \right\} \right\} < 0 \quad (3.22)$$

Substituting Equation (4.14) into Equation (4.20) and rearranging the equation, yields the following.

$$\Rightarrow -s \left\{ \frac{\text{sign}(s)}{k} \right\} < 0 \quad (3.23)$$

From the above equation(Equation 4.21) we can extract the conditions that should be fulfilled for the stability of the system.

1.  $S \text{sign}(S) = |S|$  , this implies that  $S \text{sign}(S)$  is always a positive quantity.
2. To have a stable system  $k$  should be a positive gain.

# Chapter 4

## Simulation Studies

### 4.1 Introduction

In this chapter, the numerical parameters that are used for evaluating the performance of the designed controller are introduced. After the formation of the sets of the initial conditions, the results of the performed computer simulations are presented in the form of tables and figures. Finally, the results will be discussed in term of the selected parameters for comparison.

### 4.2 Simulation Parameters

The value of the desired wheel slip for dry concrete, dry nominal and dry slippery road types are selected as -0.2, -0.175 and -0.15 respectively by considering that the peak value of tractive force occurs respectively at 20%, 17.5% and 15% slip for most surfaces. The computer simulations were carried about with the initial condition of the vehicle velocity set to  $40\text{km/h}$ ,  $90\text{km/h}$ ,  $150\text{km/h}$  and the braking is occurred on dry concrete, dry nominal and dry slippery road. Outputs of the system which have been used to evaluate the performance of the controller proposed are the actual slip, the stopping distance, the wheel speed, and the vehicle velocity. The parameter used in the simulation was adapted from [30]. During our simulation of ABS without SMC, the basic inputs for controlling the vehicle are the engine torque and the breaking torque. For a dry concrete and slippery road with a vehicle initial speed of  $40\text{km/h}$ ,  $90\text{km/h}$  and  $150\text{km/h}$ , the engine torque considered is  $501.7\text{Nm}$ ,  $222.99\text{Nm}$  and  $133.794\text{Nm}$  respectively. Whereas for a dry nominal road, for all initial vehicle speeds, the engine torque considered is  $2000\text{Nm}$ . In addition to the engine torque, the braking torque /an exhaust brake/ is a means of slowing a diesel engine by closing off the exhaust path from the engine, causing the exhaust gases to be compressed in the exhaust manifold, and in the cylinder. Since the exhaust is being compressed, and there is no fuel being applied, the engine works backwards, slowing down the vehicle. The amount of negative torque generated is usually directly proportional to the back pressure of the engine. An exhaust brake is a device that essentially creates a major restriction in the exhaust

system, and creates substantial exhaust back pressure to retard engine speed and offer some supplemental braking. As it is shown in Table 4.2, The braking torques are generated from the system dynamics.

Table 4.1: system parameters [28].

Symbol	Description	Value
$J_w$	Moment of inertia of wheel	$3kg - m^2$
$M_t$	Mass of the quarter vehicle	637.5 kg
$M_v$	Vehicle mass	2550 kg
g	Gravitational constant	$9.81m/s^2$
$R_w$	Wheel radius	0.326 m
$N_w$	Total number of wheel during braking	4
$A_f$	Frontal area of the vehicle	$3.03705m^2$
$\rho$	Air density	$1.184 kg/m^3$
$C_d$	Aerodynamic drag coefficient	0.36
L	Wheel base	2.985 m
l	Overall length of the vehicle	4.715 m
w	Overall width of the vehicle	1.8 m
h	Overall height of the vehicle	1.985 m
$h_{cg}$	Center of gravity height	0.46 m
C	<b>Coefficient of friction</b> $\Rightarrow$ For Dry concrete road $\Rightarrow$ For Dry nominal road $\Rightarrow$ For Dry slippery road	0.8 0.75 0.2

At it is shown in Table 4.2, both the peak value of adhesion coefficient and wheel slip are control parameters for ABS with and without SMC.

Table 4.2: Control parameters

ABS with and without SMC		
Symbol	Description	Value
$\mu_p$	<b>Peak value of the adhesion coefficient</b>	
	$\Rightarrow$ For Dry concrete road	0.8
	$\Rightarrow$ For Dry nominal road	0.5
	$\Rightarrow$ For Dry slippery road	0.2
$\lambda_p$	<b>Peak value of the wheel slip</b>	
	$\Rightarrow$ For Dry concrete road	0.2
	$\Rightarrow$ For Dry nominal road	0.175
	$\Rightarrow$ For Dry slippery road	0.15
ABS with SMC		
<b>K</b>	<b>Gain of the sliding surface</b>	
	*For Dry concrete road	0.81
	* For the dry normal and slippery roads	0.83
ABS without SMC		
Engine torque	<b>For dry concrete and slippery</b>	
	$\Rightarrow$ For 40km/h	501.7Nm
	$\Rightarrow$ For 90km/h	222.99Nm
	$\Rightarrow$ For 150km/h	133.79Nm
	<b>For dry nominal</b>	2000Nm
Braking torque	$T_b = m * a * R_w$	

### 4.3 Simulation Results and Discussions

After constructing the brake system and control system model and setting the initial conditions, the computer simulations are carried out by formulating a program using MATLAB for all the configurations and scenarios defined above. Performing the relevant computer simulations for each of these situations separately, the corresponding stopping distance and the required braking time values are determined as given in Table 4.3. From this table we can see that the SMC based ABS was faster than ABS without SMC for all initial velocity of the vehicle and road types.

Table 4.3: Stopping distance and braking time Results obtained from ABS simulation with and without SMC

Type of Road	Initial Velocity of the Vehicle (km/hr)	Initial Angular velocity of the wheel (rad/s)	ABS without SMC		SMC based ABS	
			Braking time (s)	Stopping distance(m)	Braking time (s)	Stopping distance(m)
Dry concrete	40	34.08	1.93	10.7280	1.88	9.7629
Dry nominal	40	34.08	2.83	15.7080	2.72	14.5000
Dry slippery	40	34.08	10.3	57.3581	6.1	33.3935
Dry concrete	90	76.68	4.15	51.9443	4.08	49.5997
Dry nominal	90	76.68	6.36	79.6029	5.97	73.5122
Dry slippery	90	76.68	18.57	231.854	13.53	169.0943
Dry concrete	150	127.8	6.82	142.2551	6.7	137.8821
Dry nominal	150	127.8	10.59	221.1023	9.84	204.2759
Dry slippery	150	127.8	29.02	608.6661	22.23	469.6940

Table 4.4: Slip results obtained from ABS simulations and with and without SMC

Type of Road	Linear Velocity	Angular velocity	Slip of ABS without SMC	Slip of ABS with SMC
Dry concrete	40	34.08	-0.13	-0.2
Dry nominal	40	34.08	-0.12	-0.175
Dry slippery	40	34.08	-0.045	-0.15
Dry concrete	90	76.68	-0.145	-0.2
Dry nominal	90	76.68	-0.12	-0.175
Dry slippery	90	76.68	-0.055	-0.15
Dry concrete	150	127.8	-0.145	-0.2
Dry nominal	150	127.8	-0.11	-0.175
Dry slippery	150	127.8	-0.06	-0.15

As we can see from Table 4.3 and 4.4, in all conditions the sliding mode controller based antilock braking system have achieved a better performance than that of the ABS system. This achieves our goal of the thesis. The performance of the controller that will be investigated in this study is assigned by the three parameters, namely, the wheel slip, vehicle and wheel speed, and the stopping distance.

Figures 4.1 to 4.12 show the simulation results of ABS based on sliding mode controller that was developed using MATLAB with the various initial condition of the vehicle velocity. These various initial velocities are set from low to high speed 40 km/h, 90 km/h and 150 km/h. Different road conditions have been simulated by using different  $\mu_p$  and  $\lambda_p$  in the function of  $\mu(\lambda) = \frac{2\mu_p\lambda_p\lambda}{\lambda_p^2 + \lambda^2}$ . Simulations are performed on a dry concrete road ( $\mu_p = 0.8, \lambda_p = 0.2$ ) and slippery road ( $\mu_p = 0.2, \lambda_p = 0.15$ ) and we chose nominal road conditions for control design purposes such that the adhesion coefficient and wheel slip peak values would be the average of the values for extreme conditions ( $\mu_p = 0.5, \lambda_p = 0.175$ ) [14].

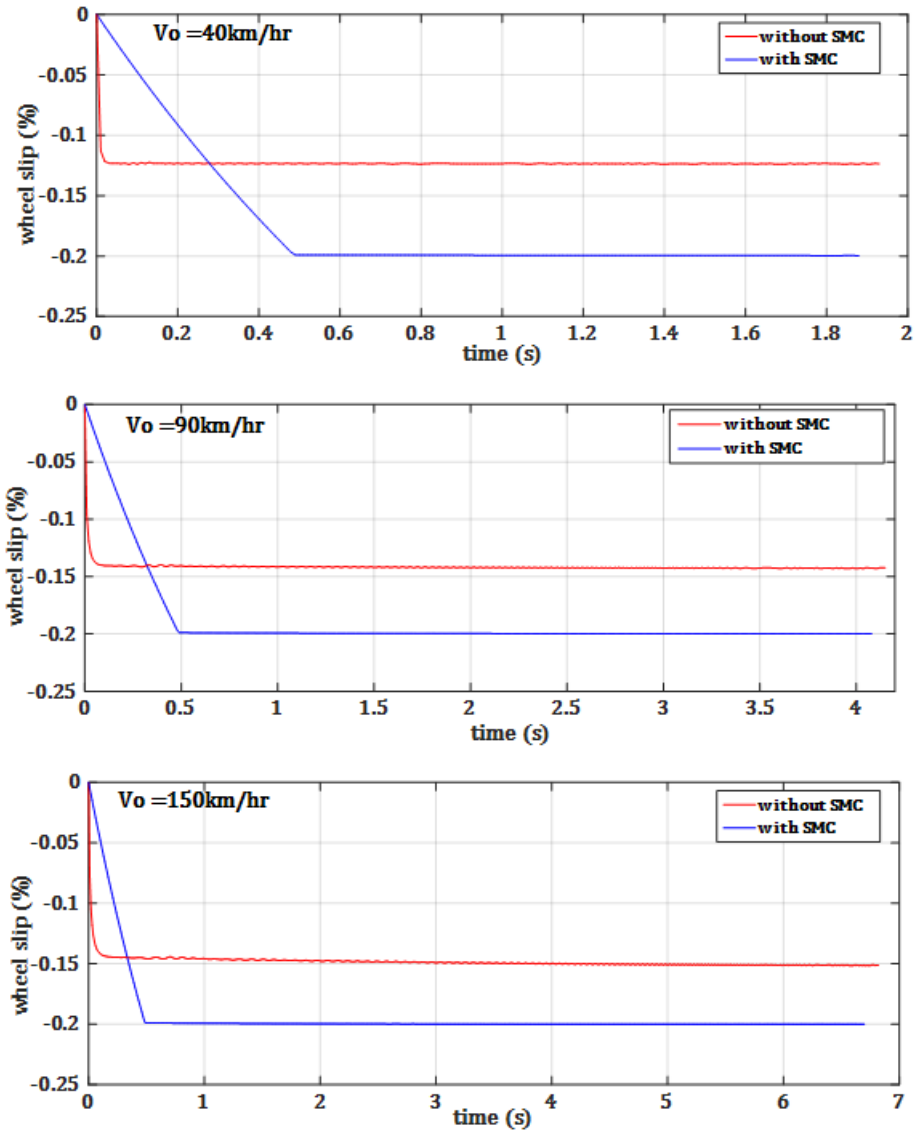


Figure 4.1: Wheel slip response of the ABS with and without SMC with various initial speeds for dry concrete road

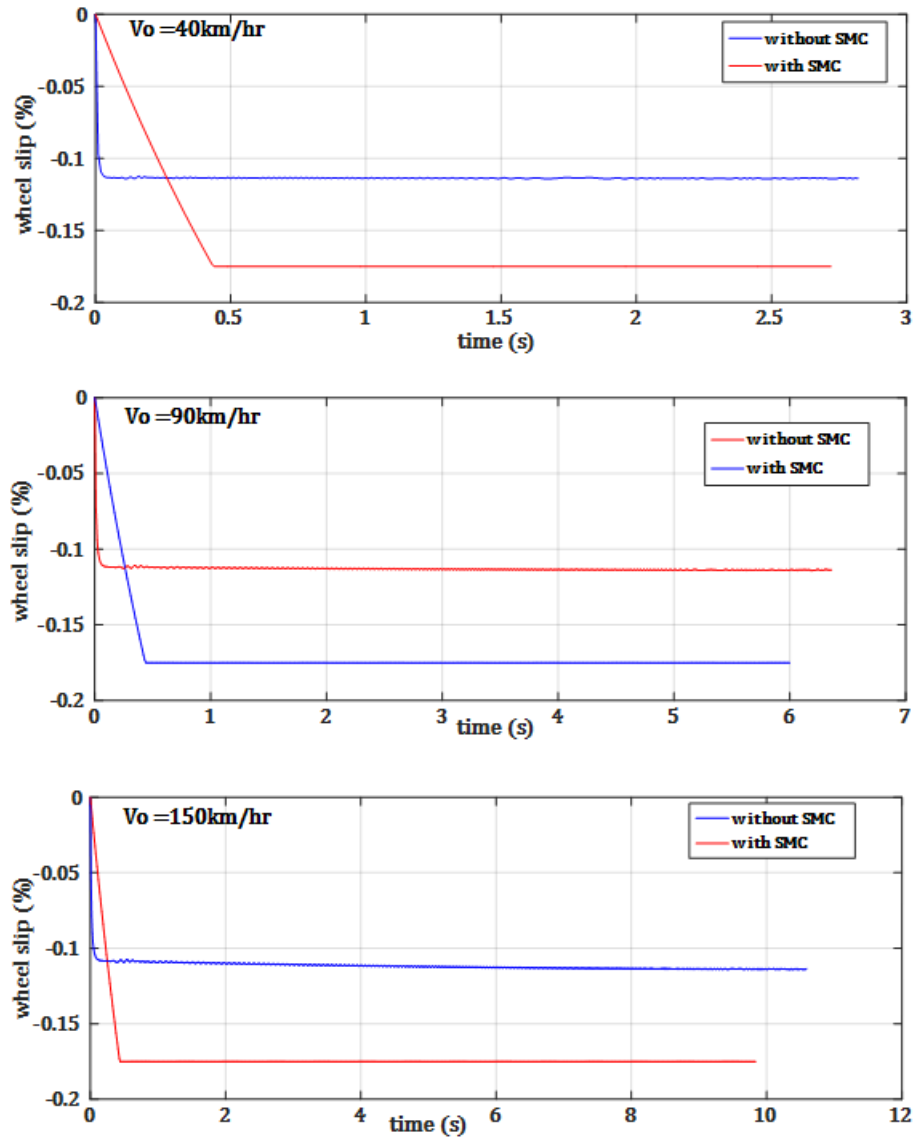


Figure 4.2: Wheel slip response of the ABS with and without SMC with various initial speeds for dry nominal road

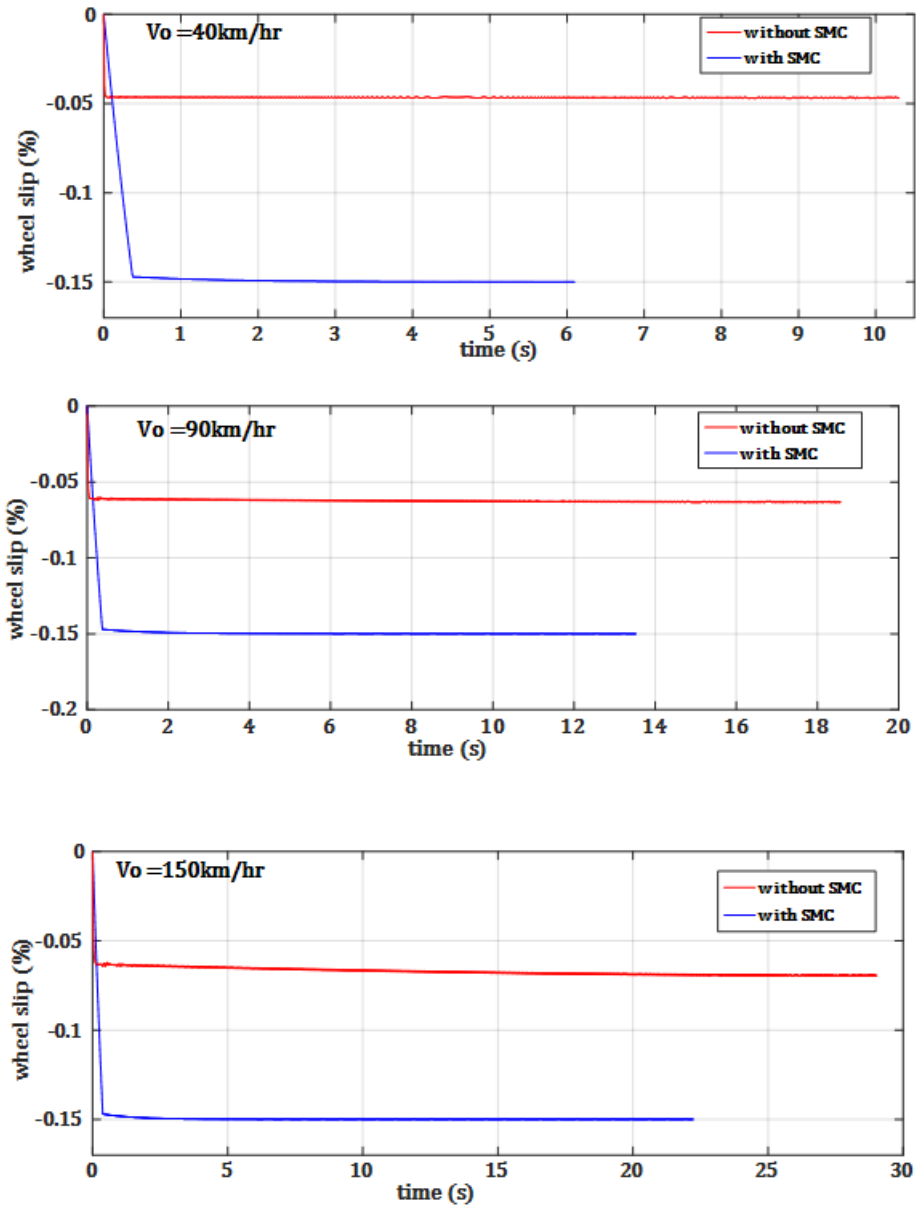


Figure 4.3: Wheel slip response of the ABS with and without SMC with various initial speeds for dry slippery road

Figure 4.1 to 4.3 shows the plot of the wheel slip response of the antilock braking system with and without SMC for various initial condition of the vehicle velocity and road type. For the SMC based ABS system, it is seen that the output follows the desired wheel slip trajectory (for dry concrete road= -0.2, for dry nominal road = -0.175 and for dry icy road = -0.15). It means that the designed controller can maintain the wheel slip in the peak value of the  $\mu$ - slip curve. Whereas, in all road conditions and scenarios the ABS system without SMC will not track the desired trajectory.

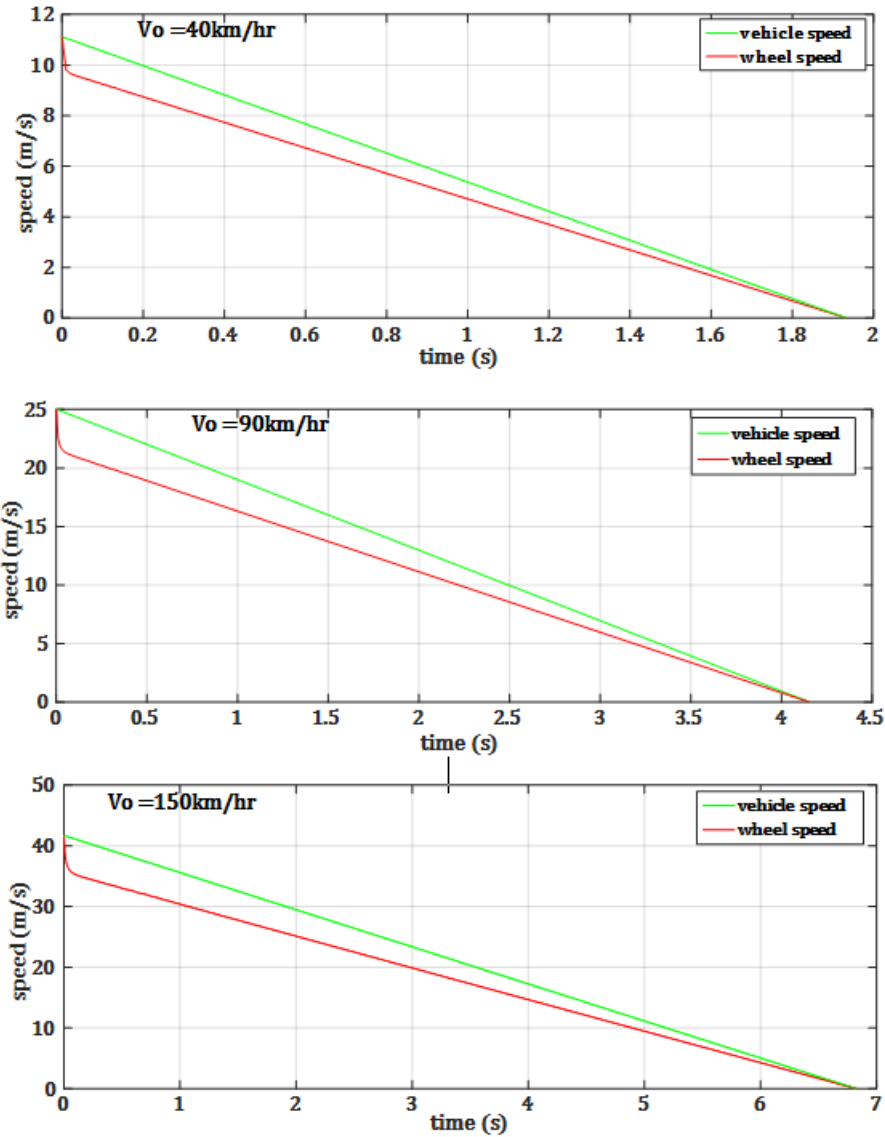


Figure 4.4: Vehicle and wheel speed response of the ABS without SMC with various initial speeds for dry concrete road

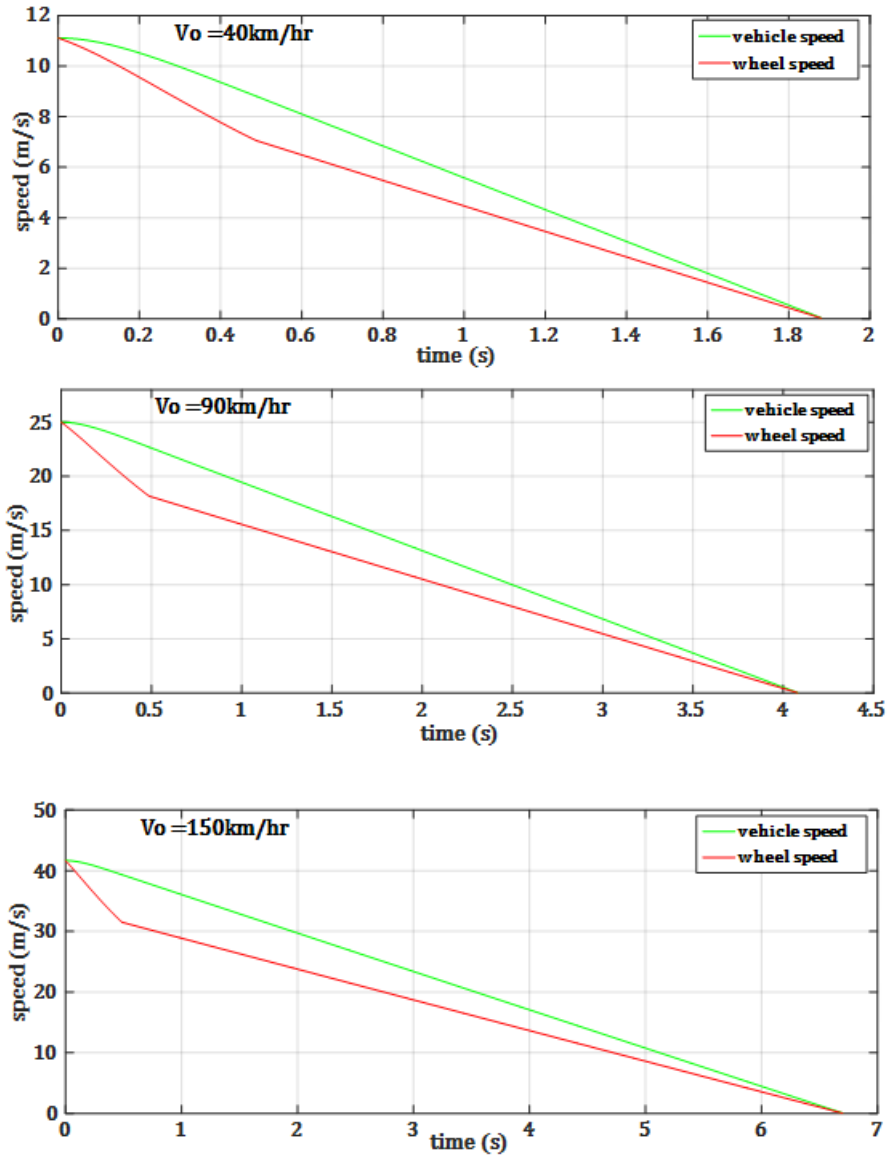


Figure 4.5: Vehicle and wheel speed response of SMC based ABS with various initial speeds for dry concrete

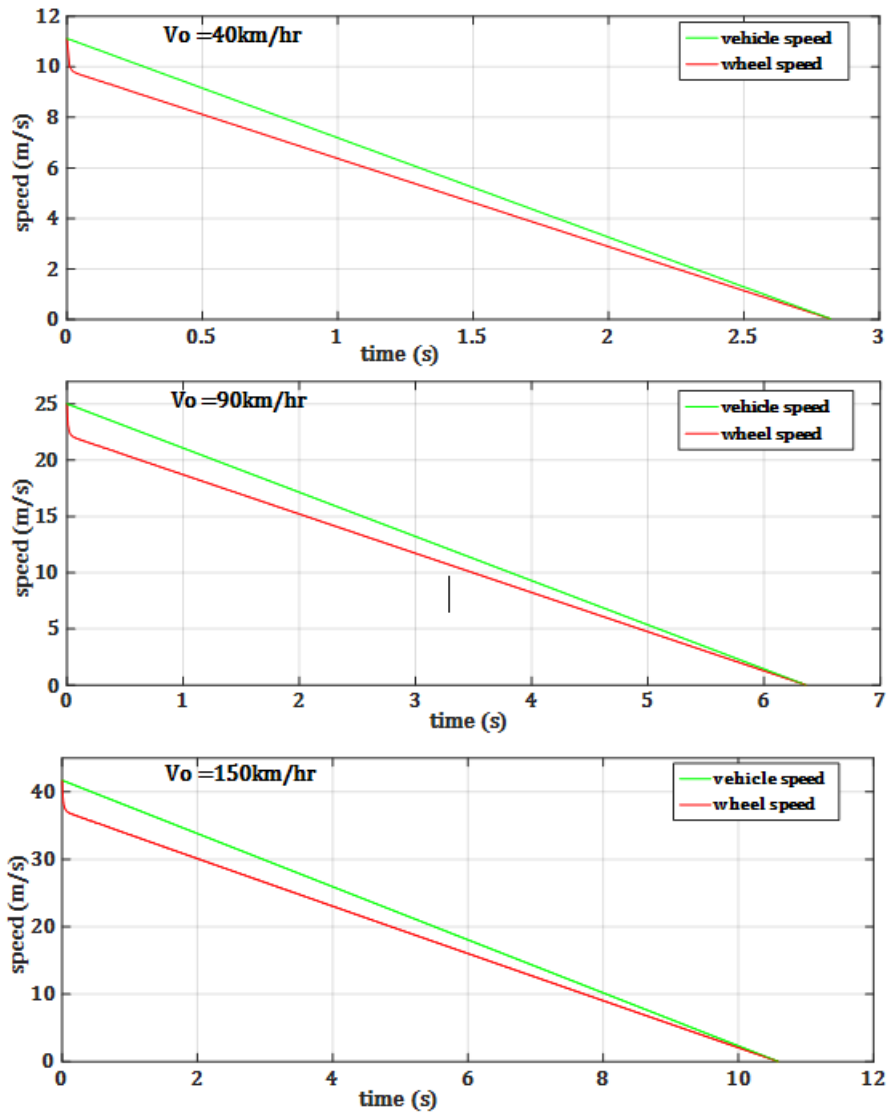


Figure 4.6: Vehicle and wheel speed response of the ABS without SMC with various initial speeds for dry nominal road

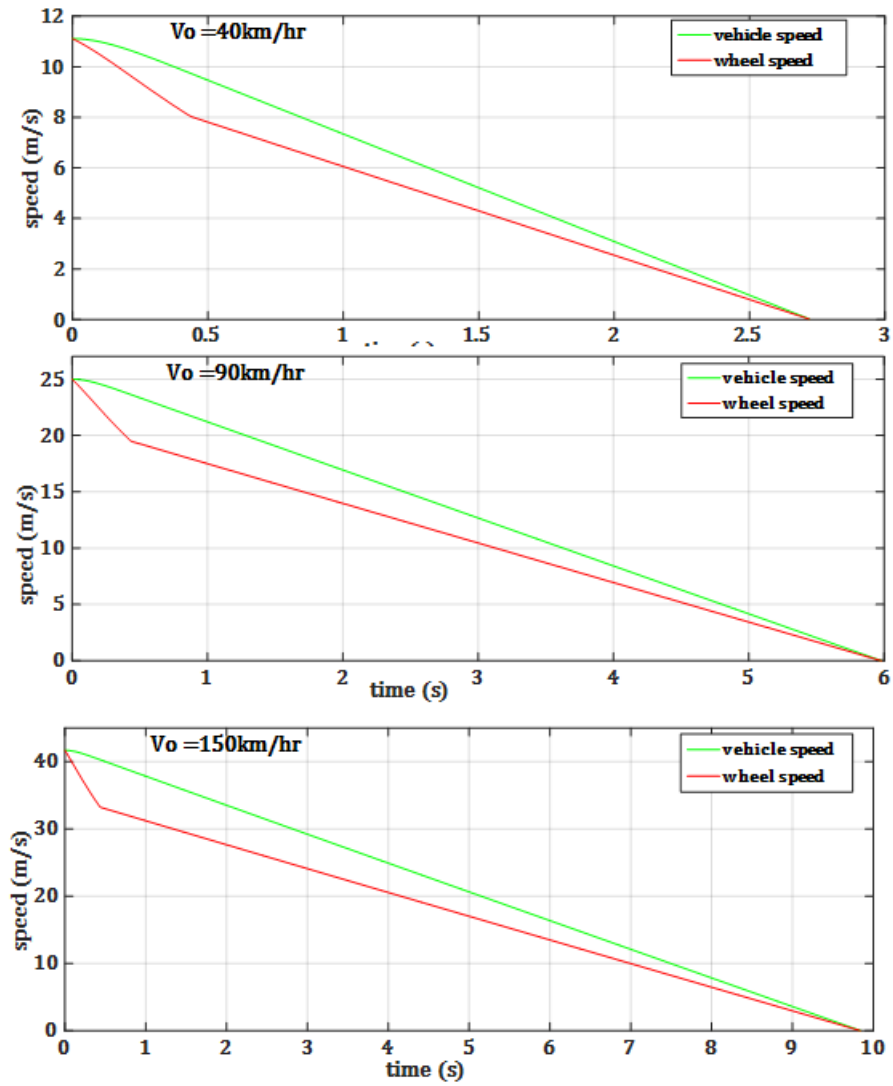


Figure 4.7: Vehicle and wheel speed response of SMC based ABS with various initial speeds for dry nominal road

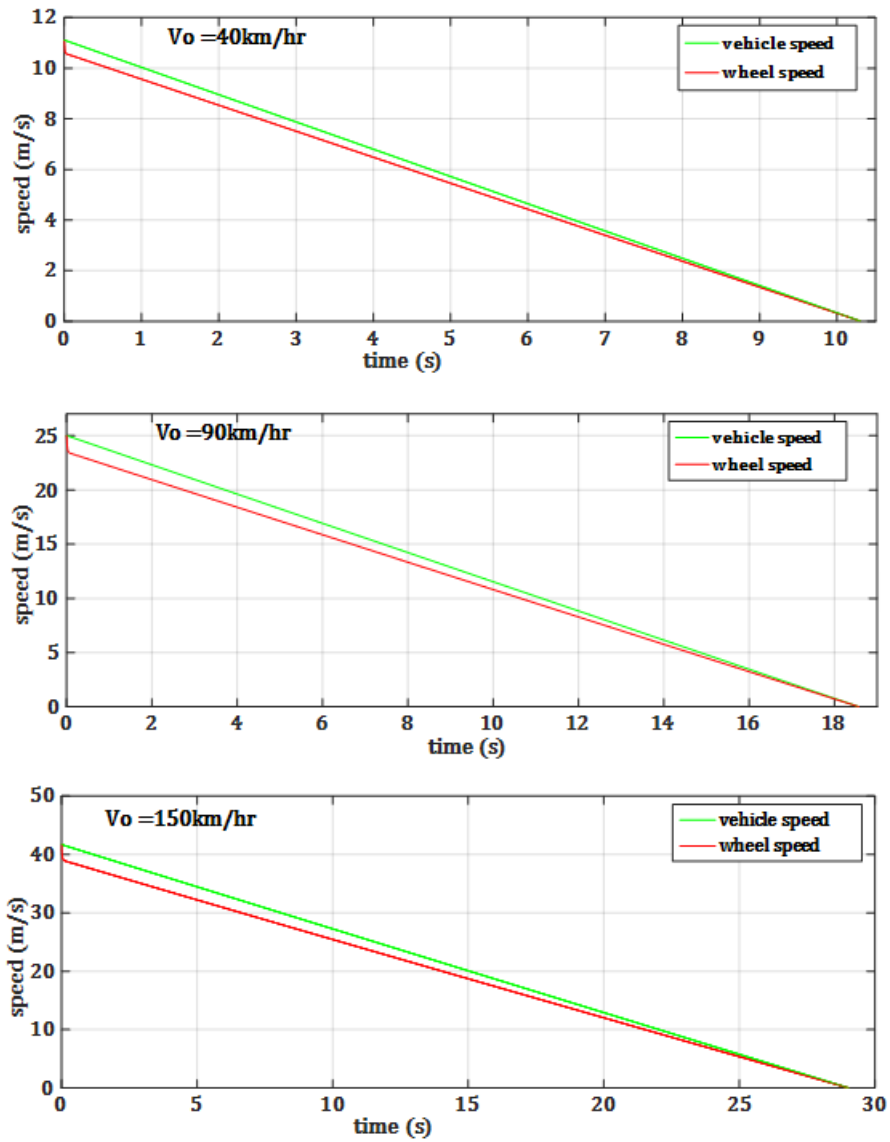


Figure 4.8: Vehicle and wheel speed response of the ABS without SMC with various initial speeds for slippery road

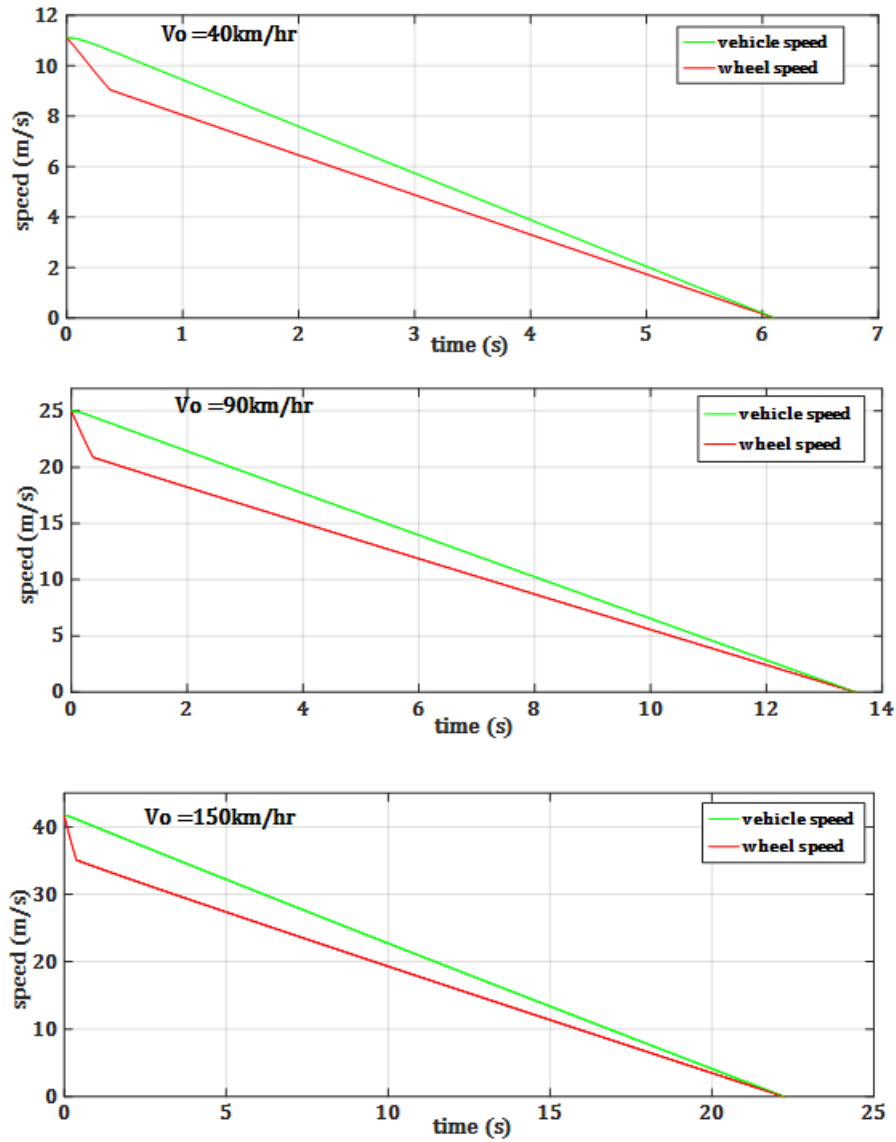


Figure 4.9: Vehicle and wheel speed response of SMC based ABS with various initial speeds for slippery road

Figure 4.4 to 4.9 illustrates the plot of vehicle and wheel speed response with the various initial condition of the vehicle velocity and different surface. The value of the wheel speed is always less than to as that of the value of the vehicle speed and it never reaches zero value until the vehicle stops. This phenomenon shows that the wheel is never fully lockup during braking. Thus, ABS shows to work properly using the proposed sliding mode controller. The plot of stopping distance with the various initial condition of the vehicle velocity can be seen in Figure 4.10 to 4.12. The simulation that was carried out with the initial condition of the vehicle velocity set to  $40\text{km/h}$ ,  $90\text{km/h}$  and  $150\text{km/h}$  generated the stopping distance with varies road type as shown in Table 4.3. The stopping distance will increase as goes concrete to slippery road. This implied that the value of the adhesion coefficient increases as the stopping distance decreases.

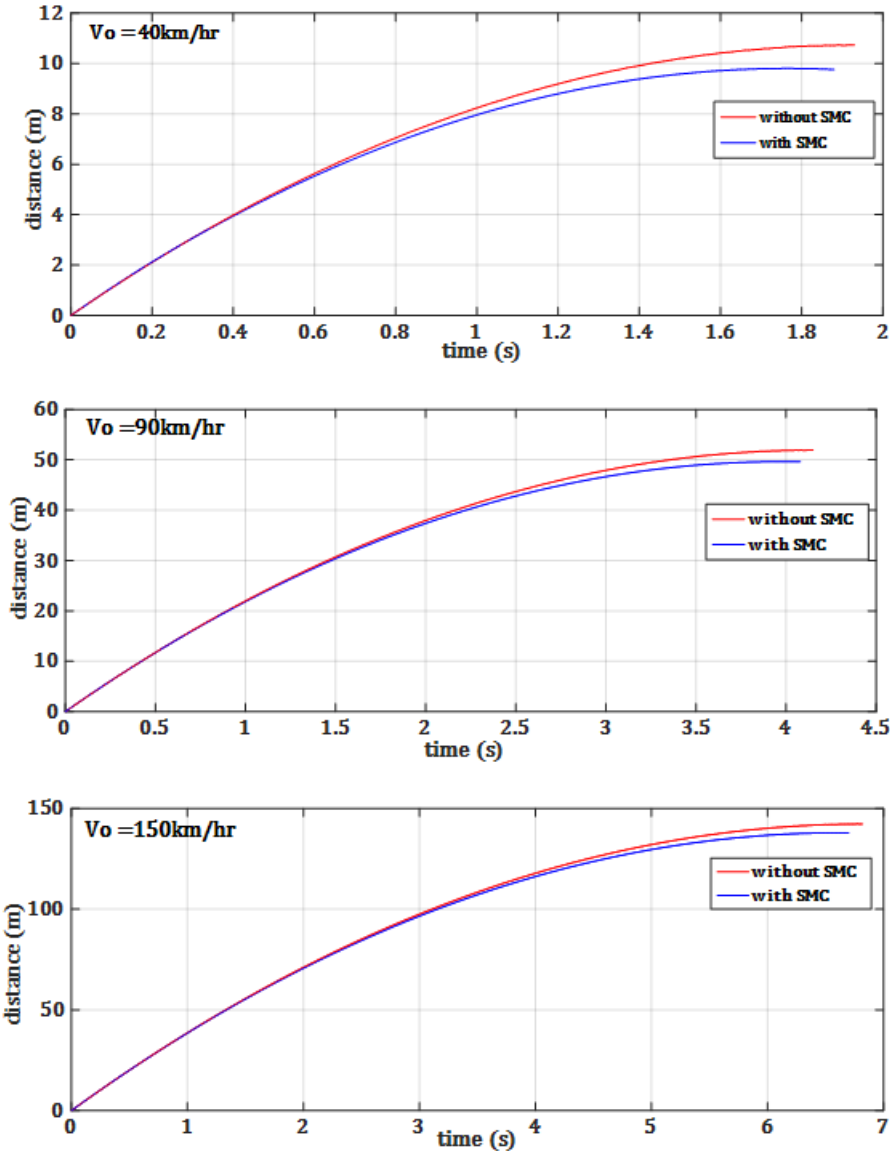


Figure 4.10: Stopping distance of the ABS with and without SMC with various initial speeds for dry concrete road

As it is shown in Figure 4.10, the SMC based ABS of a vehicle on the dry concrete road with an initial vehicle speed of 40 km/h, 90 km/h and 150 km/h generated a stopping distance of 9.7629m, 49.5997m and 137.8821m respectively. Whereas, for the same initial speeds of the vehicle on the dry concrete road surface, the ABS without SMC generated a stopping distance of 10.7280 m, 51.9443m and 142.2551m respectively. As we can see from the numeric values on the two cases, the higher initial speed applied the longer stopping distance was resulted. In addition, as it is shown in Table 4.3 also, the braking time of SMC based ABS is faster than to that of ABS without SMC. From this we can conclude that SMC based ABS is more decelerate than ABS without SMC for Dry concrete road.

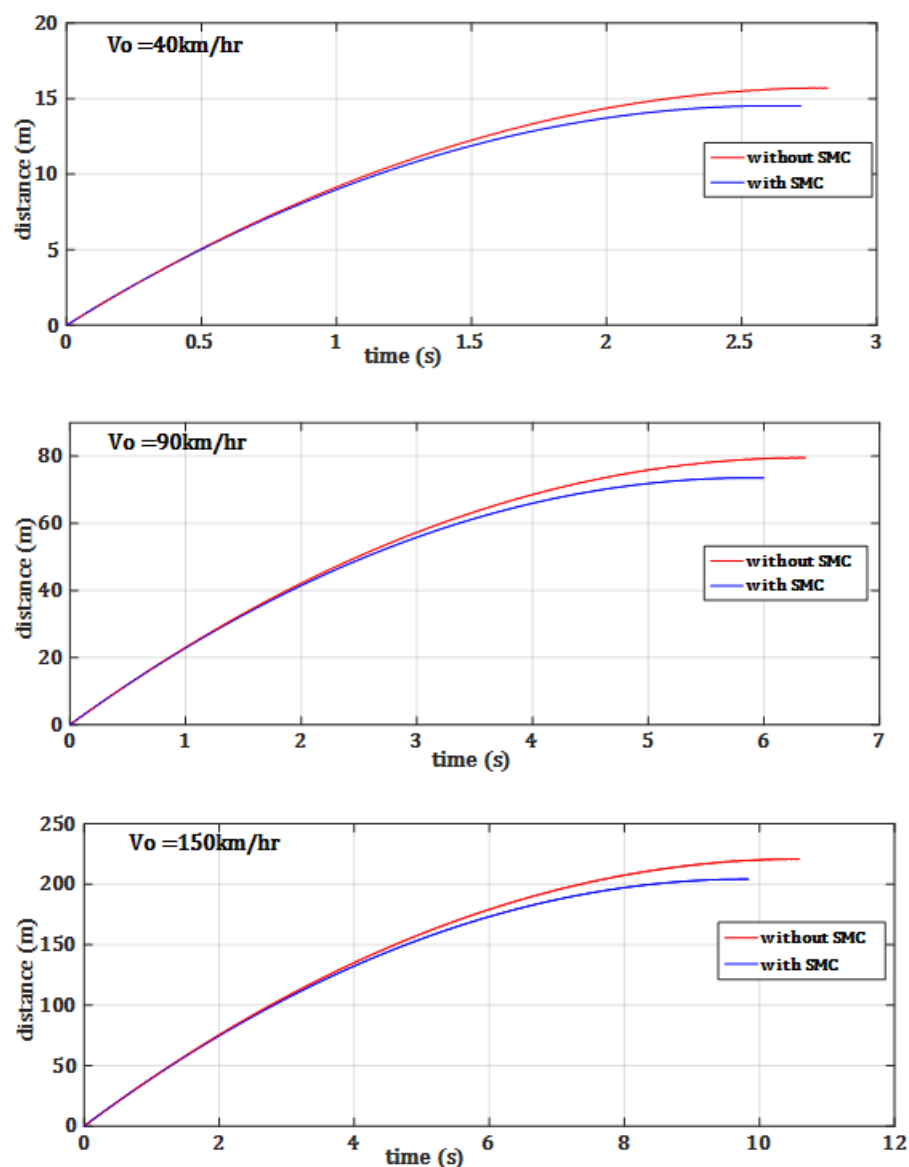


Figure 4.11: Stopping distance of the ABS with and without SMC with various initial speeds for nominal road

Figure 5.11 shows the simulation result for nominal road. The simulation that was carried out with the initial condition of the vehicle velocity set to 40 km/h, 90 km/h and 150 km/h generated the stopping distance with a value of 15.7080 m, 79.6029m and 221.1023m ABS with out SMC and 14.5000m, 73.5122m and 204.2759m ABS with SMC respectively. And also we can see that the braking time of ABS with out SMC is much slower than SMC based ABS as shown in Table 4.3. From this we can conclude that SMC based ABS is more decelerate than ABS with out SMC for dry nominal road. The higher initial speed applied the longer stopping distance was resulted also.

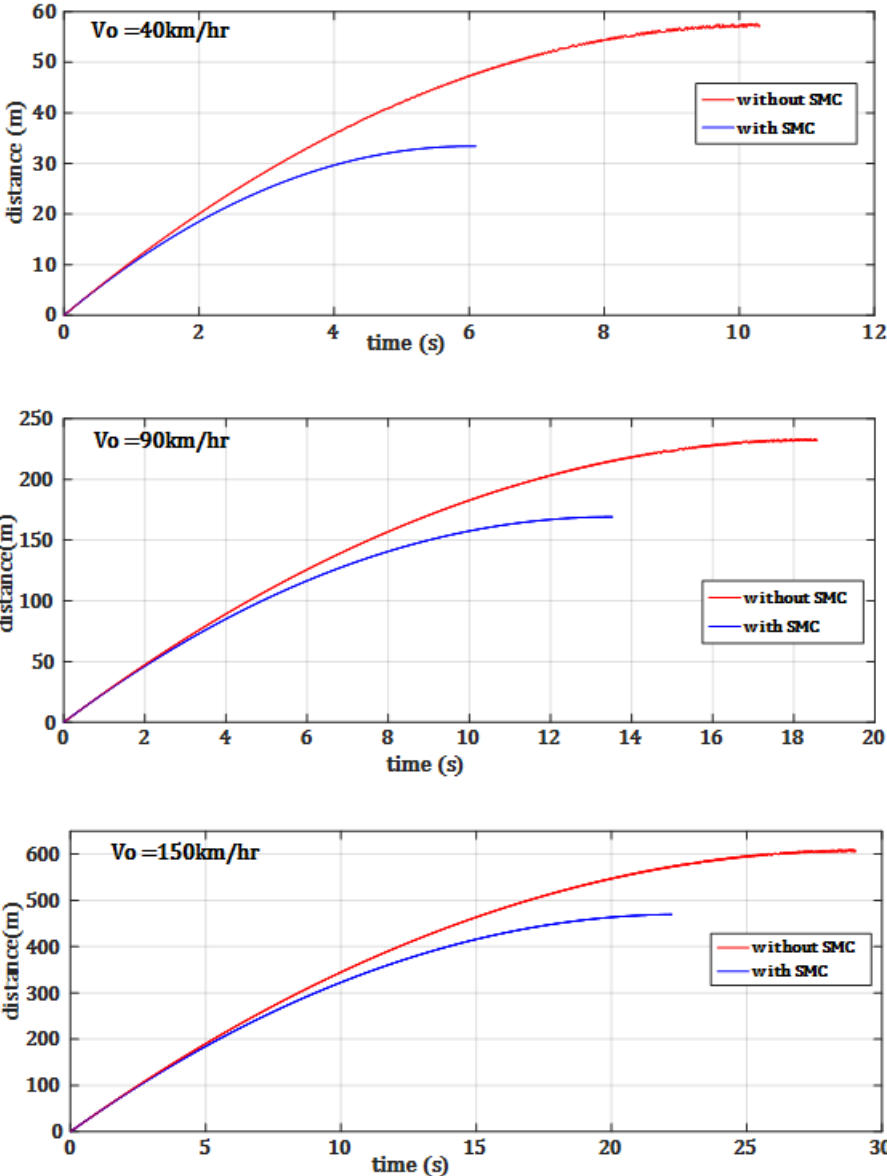


Figure 4.12: Stopping distance of the ABS with and without SMC with various initial speeds for slippery road

Figure 4.12 shows the simulation result for slippery road. The simulation that was carried out with the initial condition of the vehicle velocity set to 40 km/h, 90 km/h and 150 km/h generated the stopping distance with a value of 57.3581m, 231.854m and 608.6661m ABS with out SMC and 33.3935m, 169.0943m and 469.6940m ABS with SMC respectively. And as shown Table 4.3 the braking time of SMC based ABS was faster than ABS with out SMC. From this we can conclude that SMC based ABS is more decelerate than ABS with out SMC for dry slippery road. The higher initial speed applied the longer stopping distance was resulted.

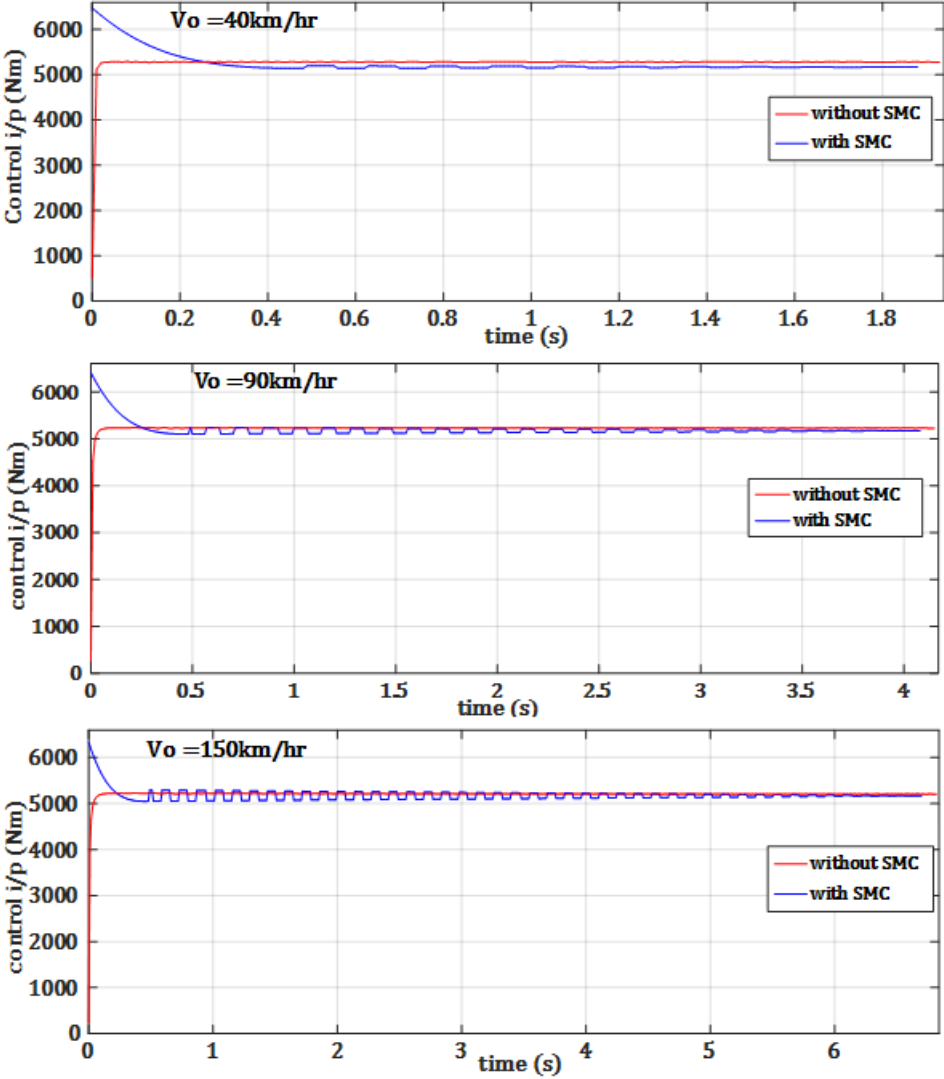


Figure 4.13: Simulation graph of control input for concrete road

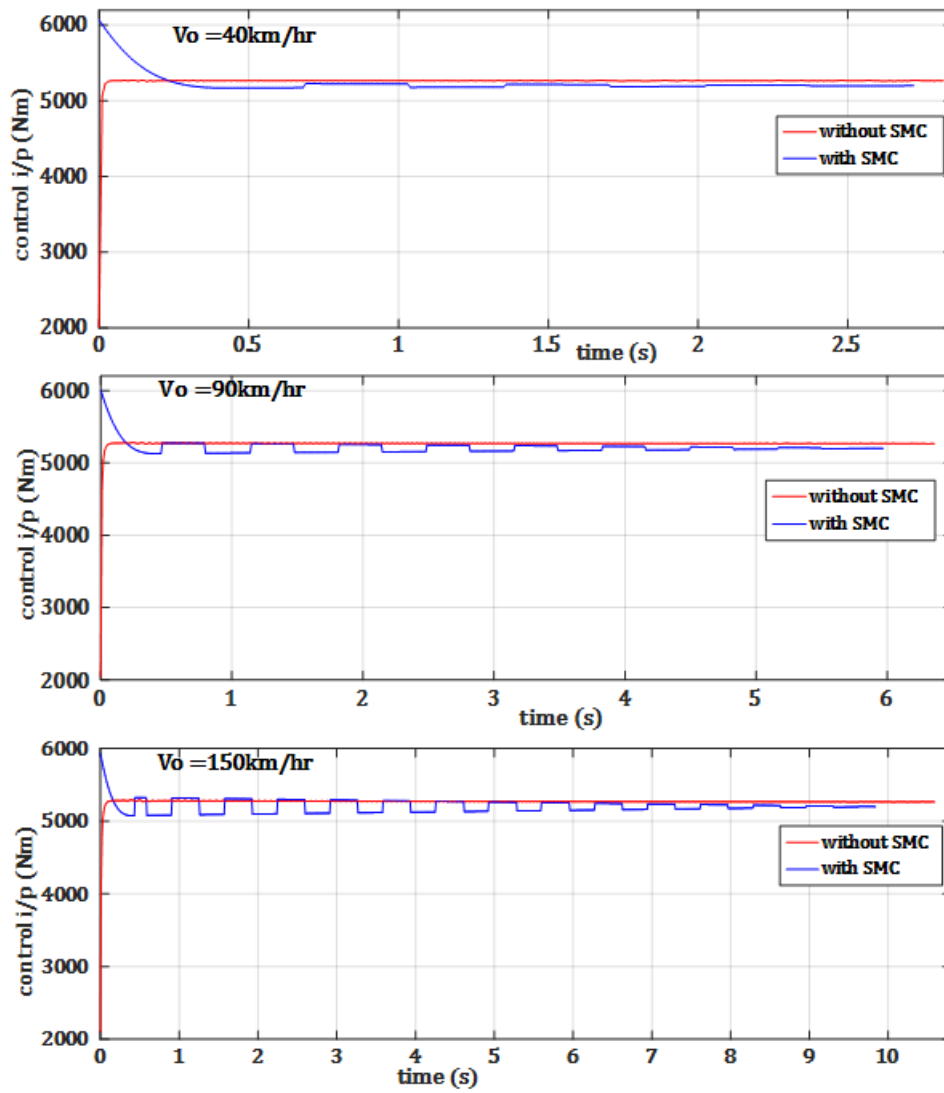


Figure 4.14: Simulation graph of control input for nominal road

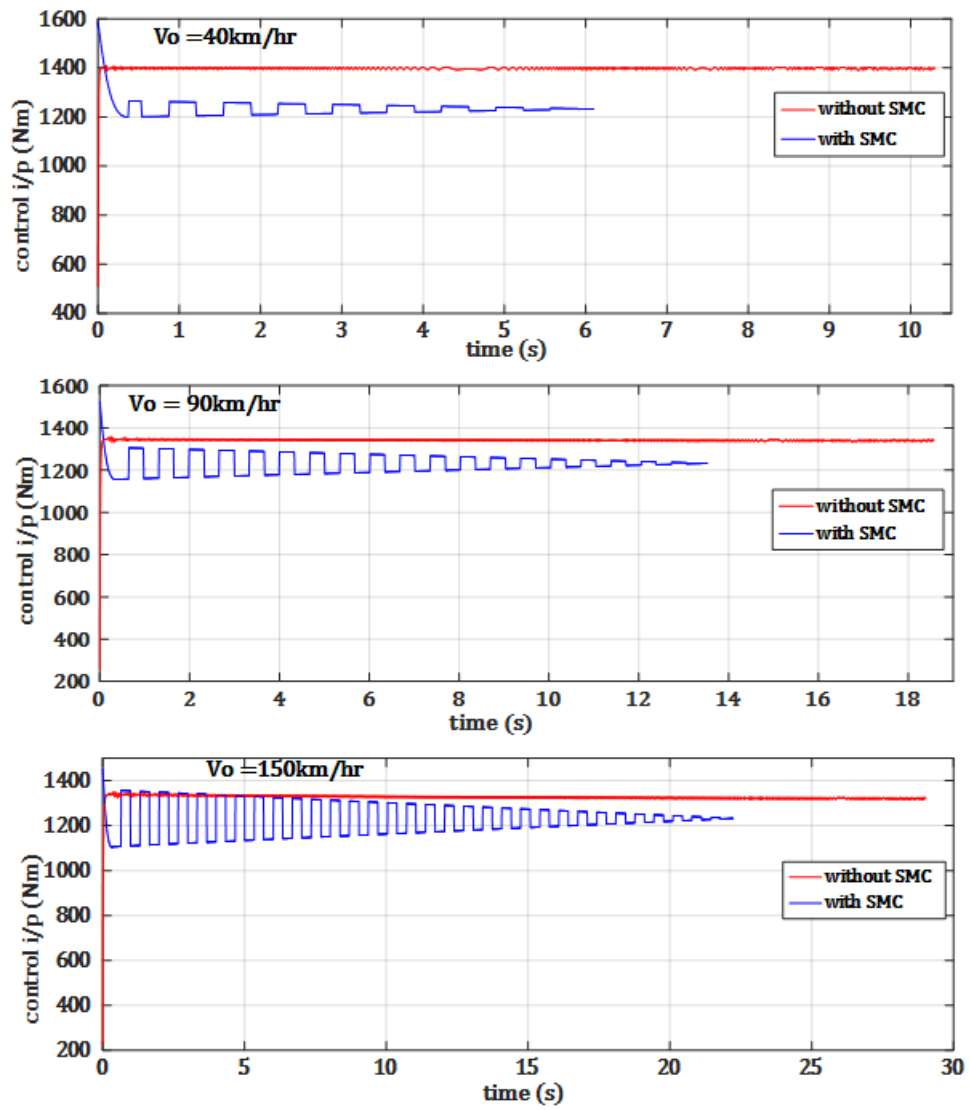


Figure 4.15: Simulation graph of control input for slippery road

As we can see from Figures 4.13 to 4.15 , the SMC based ABS exerts a less control effort than to as that of the ABS without SMC. By using this less control effort, our designed controller have already achieved its own main objective. The output in all conditions tracks the desired values.

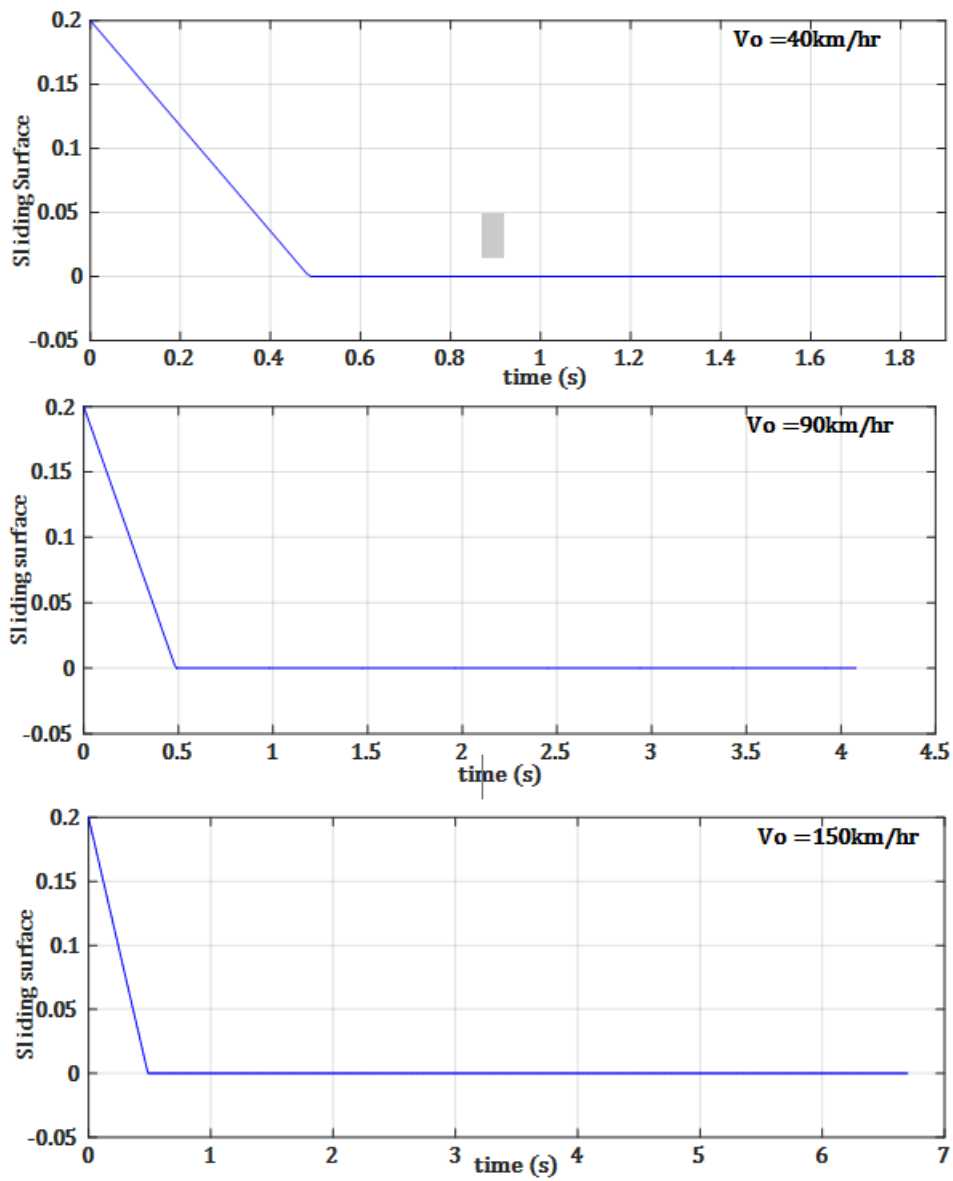


Figure 4.16: Sliding surface of SMC based ABS with various initial speeds for dry concrete road

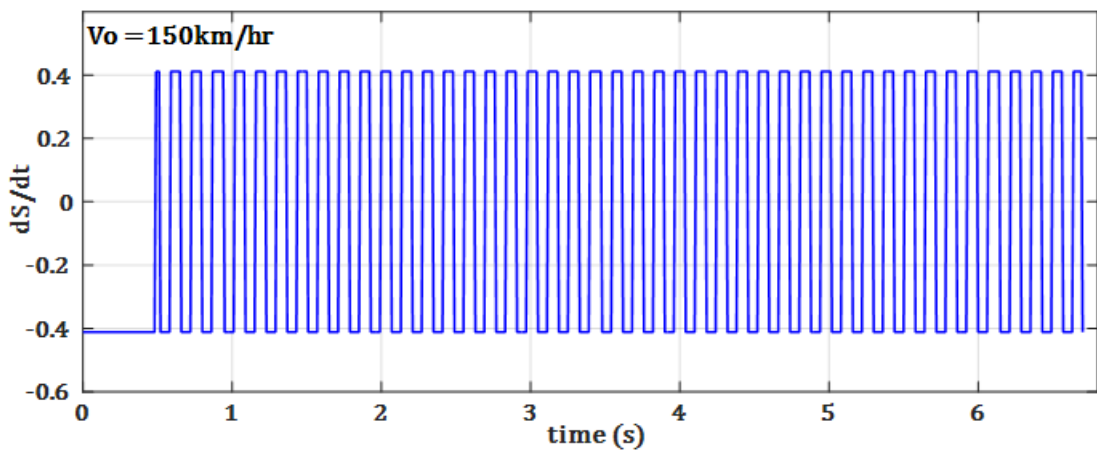
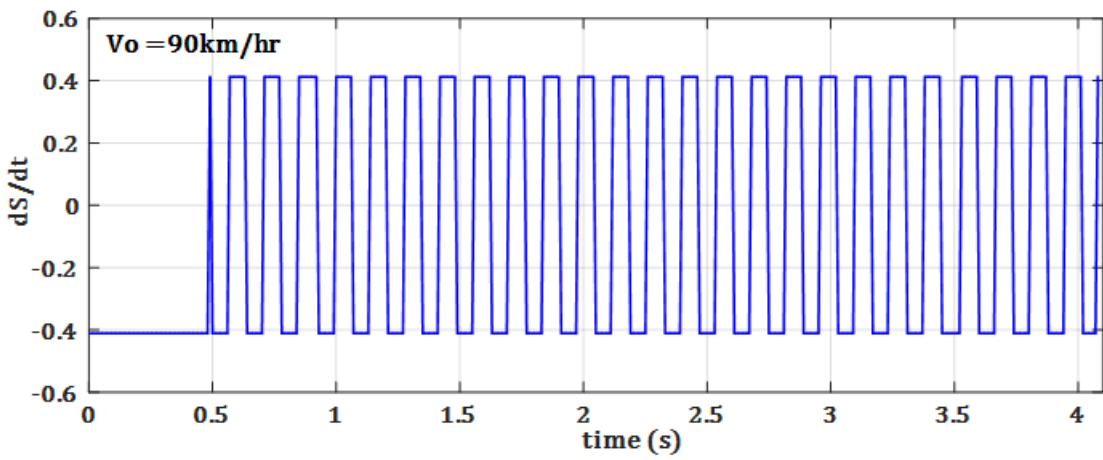
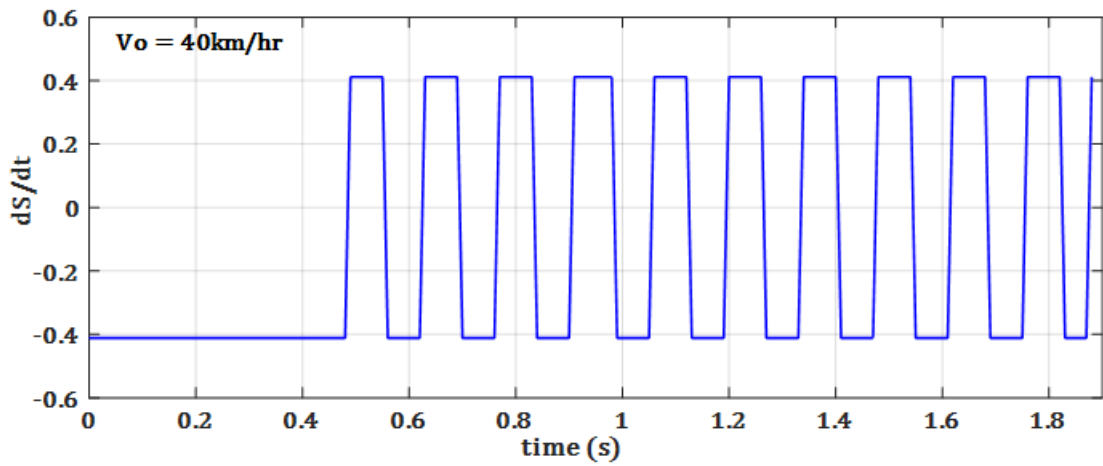


Figure 4.17: Derivative of the sliding surface of SMC based ABS with various initial speeds for dry concrete road

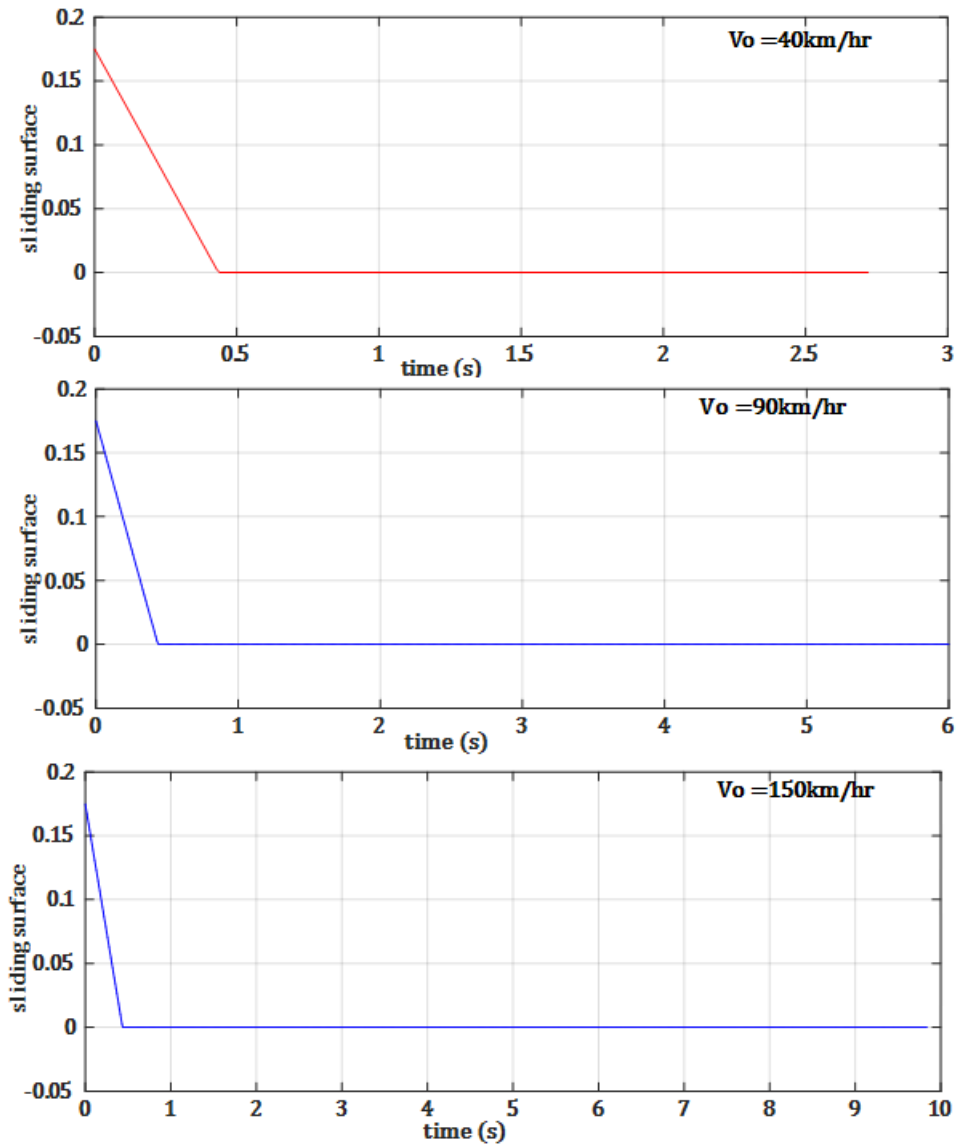


Figure 4.18: Sliding surface of SMC based ABS with various initial speeds for nominal road

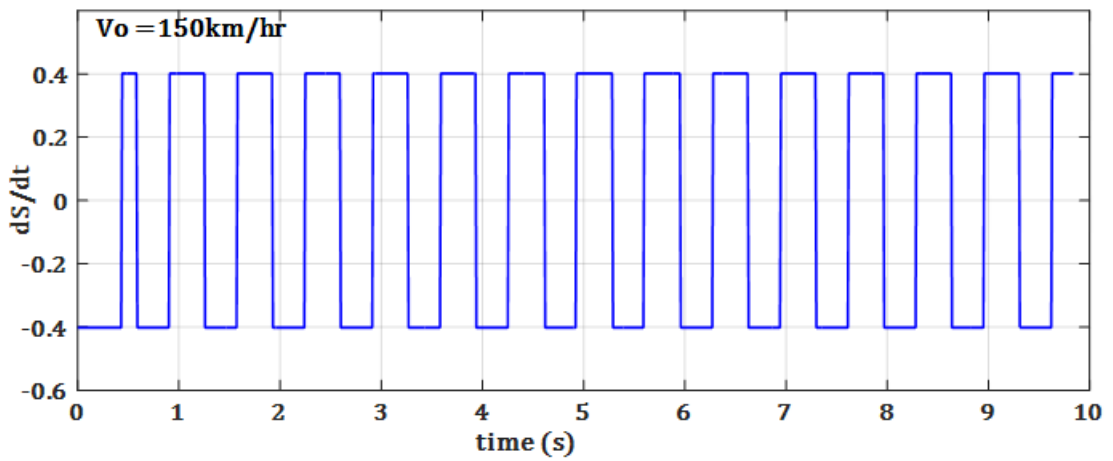
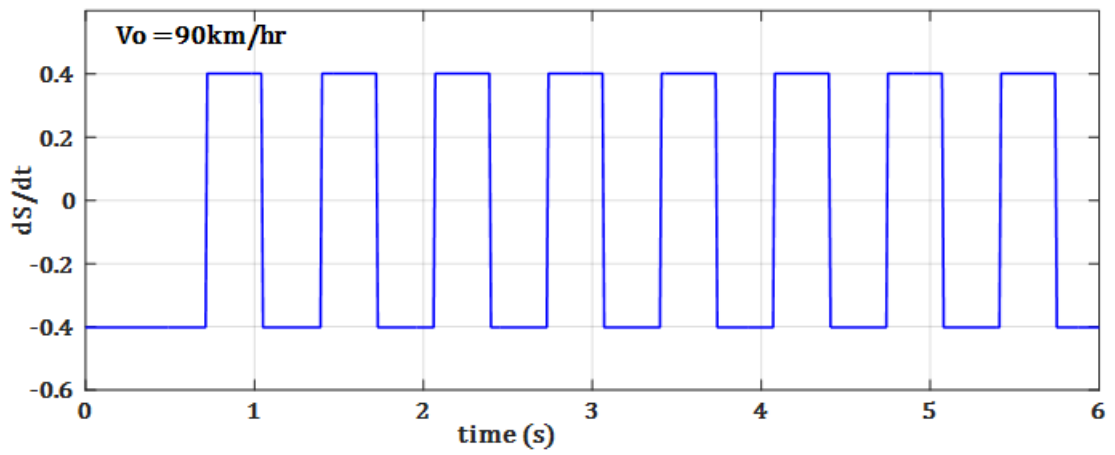
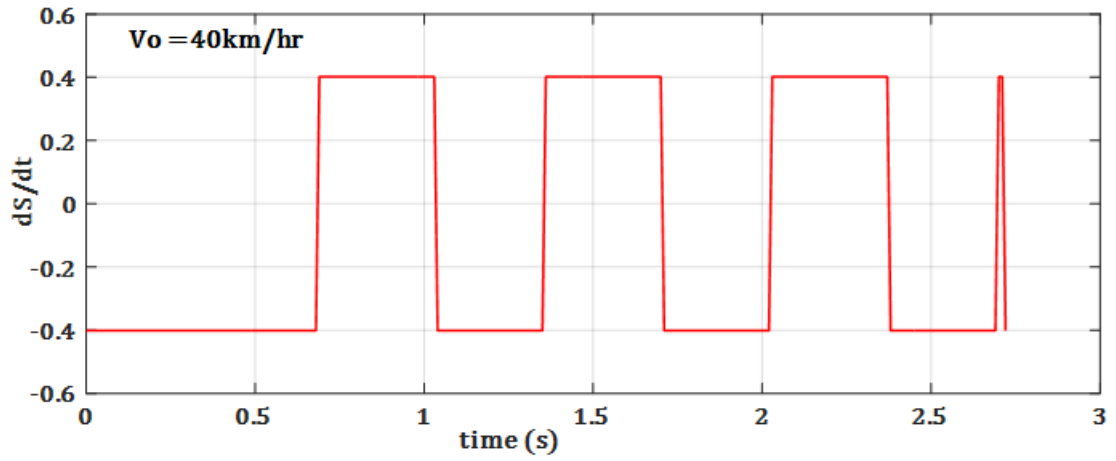


Figure 4.19: Derivative of the sliding surface of SMC based ABS with various initial speeds for nominal road

Figure 4.20: Sliding surface of SMC based ABS with various initial speeds for slippery road

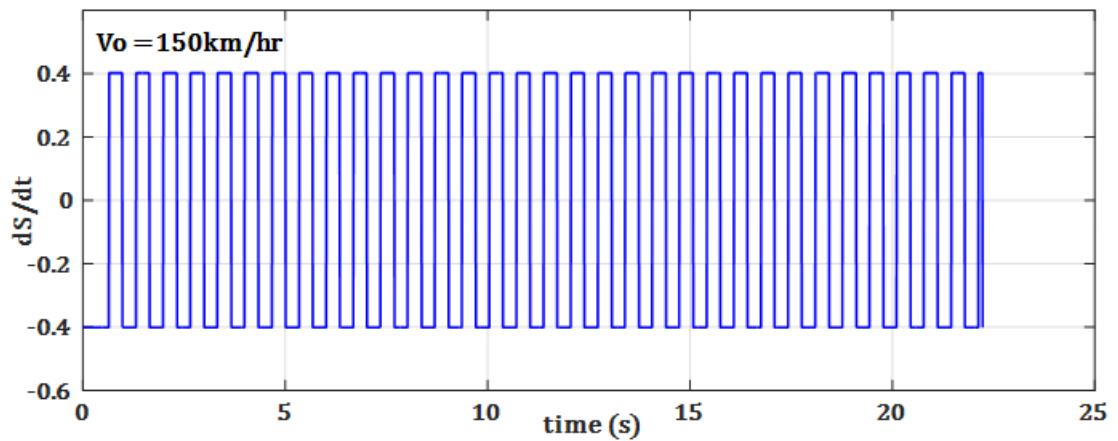
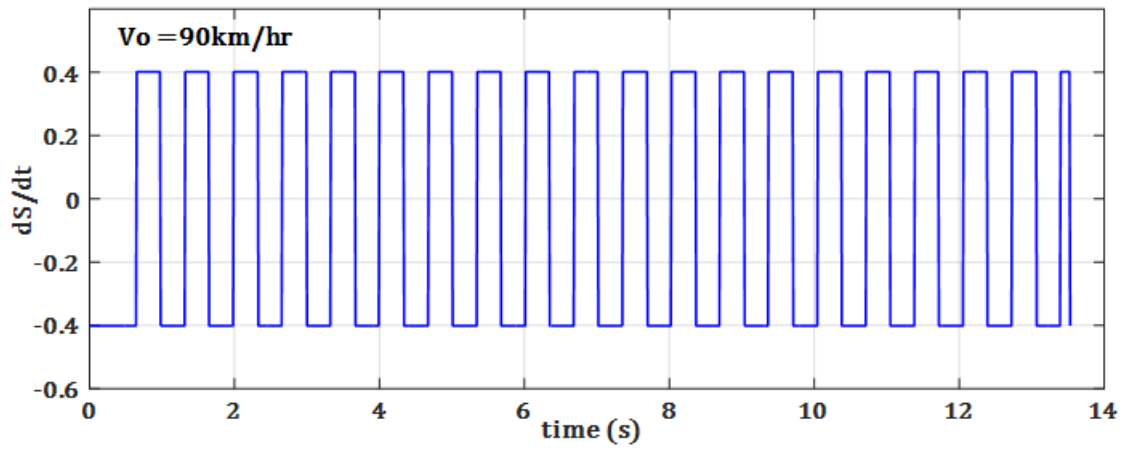
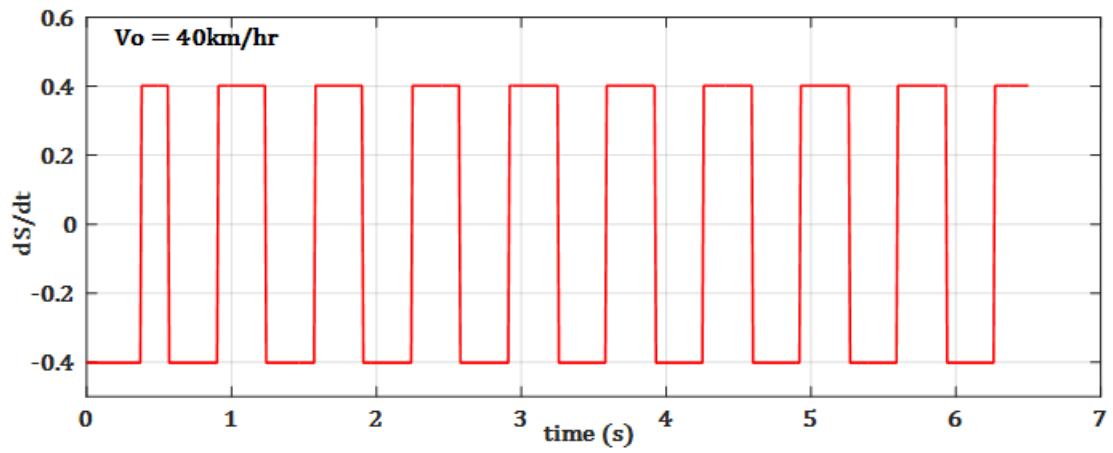


Figure 4.21: Derivative of the sliding surface of SMC based ABS with various initial speeds for slippery road

As we can understand from Figures 4.16 to 4.21, in all scenarios and road conditions, the sliding surface reaches to zero fastly before the vehicle reaches to its braking time. After the sliding surface reaches to zero, its value will remain on zero until the vehicle breaks its motion. As we can see from the derivative of the sliding surface trajectory, it is bounded by 0.4 to -0.4. Until the braking time, there isn't any unique oscillation that is observed out of this range. In general, as we can understand from the sliding surface and its derivative output trajectories, the designed system rejects chattering and creates a robust system.

# Chapter 5

## Conclusions, Recommendations and Future Works

### 5.1 Conclusions

The aim of this thesis study is to design sliding mode controller based antilock braking system for the purpose of minimizing stopping distance and stabilizing the system. The mathematical model of the antilock braking system with the nonlinear control strategy has been discussed. The ABS model which includes nonlinear characteristic and parameters uncertainties was developed based on a quarter car model.

The wheel slip is chosen as the controlled variable for the braking control algorithms. For the wheel slip control system, the vehicle and brake system are highly nonlinear and time-varying systems. That makes sliding mode controller a suitable design method for implementing the slip control system. A nominal vehicle system model is used in a MATLAB code for testing the controller performance in different road surface scenarios and initial velocity. According to the simulation results, the controller performance is satisfactory. The wheel slip is kept in the appropriate range. For evaluating and simulating the designed system, the values of the parameters are taken from [28].

The simulation that was carried out with the initial condition of the vehicle velocity set to  $40\text{ km/h}$ ,  $90\text{ km/h}$  and  $150\text{ km/h}$  generated the stopping distance for dry concretes are 9.7679m, 49.5997m and 137.8821m respectively, whereas for dry nominal roads are 14.5m, 73.5122m and 204.2759m respectively. Also the simulation that was carried out with the initial condition of the vehicle velocity set to  $40\text{ km/h}$ ,  $90\text{ km/h}$  and  $150\text{ km/h}$  the stopping distance that generates for dry slippery roads are 33.3935m, 169.0943m and 469.6940m respectively. These are the logic value for the vehicle that is driven in all road type conditions. The higher initial speed applied the longer stopping distance was resulted.

## 5.2 Recommendations

As it is shown in the result discussion part, the designed SMC based Antilock Braking System of a vehicle have shown a better result as compared to that of the conventional once. This is already validated by simulation only. So any one can take this design and it can be implemented by prototypes.

## 5.3 Suggestions for future works

As a future work,

1. The performance of SMC based antilock braking system of a vehicle can be examined under sloppy different road surfaces, like as that of curved wet concrete or nominal roads.
2. In this study, the dynamics of the system doesn't considered the actuator dynamics. Since Most anti-lock braking systems employ hydraulic valve control to regulate the brake pressure during the anti-lock operation, so anyone can develop systems by considering actuator dynamics.
3. In addition to this, when a vehicle initial velocity and vehicle type varies, our system doesn't have a mechanism for finding the gains of the sliding mode surface. So we suggest that, optimization techniques can be used for defining a variable gain and an Adaptive and intelligent control mechanisms can be augmented with the designed SMC based ABS.

# Bibliography

- [1] Altrock, C. (1994). *Fuzzy Logic Technologies in Automotive Engineering. Wescon 94, Idea/Microelectronics Conference Record. September 27 – 29.*
- [2] Bakker, E.T., Pacejka, H.B, Linder, L. (1982). *A New Tire Model with an Application in Vehicle Dynamic Studies. SAE Technical Paper No. 870421.*
- [3] Bosch, R. (1995). *Automotive Brake Systems. Cambridge, MA: Robert Bentley*
- [4] Claudio Vecchie, "*Sliding mode control: theoretical development and applications to uncertain mechanical system*"
- [5] Drakunov, S., Ozguner, U., Dix, P. and Ashrafi, B. (1994). *ABS Control Using Optimum Search Via Sliding Modes. Proc. of the 33<sup>rd</sup> Conference on Decision and Control. December. Lake Buena Vista, FL: IEEE, 479 – 85.*
- [6] Garrick F, Mark Flick, W. and Riley G. (1998). *A Comprehensive Light Vehicle Antilock Brake System Test Track Performance Evaluation. Society of Automotive Engineers. Warrendale PA.*
- [7] Getu Gabisa Tuffa, July (2011), "*Multirate Output Feedback Discrete Sliding Mode Control for an Aerial Vehicle*", *Addis Ababa Insistute of Technology, School of Graduate Studies, Addis Ababa University, Addis Ababa.*
- [8] Gillespie, T. D (1992). *Fundamentals of Vehicle Dynamics. Warrendale: Society of Automotive Engineers, Inc.*
- [9] Harnel, J.L, et al., "*Measurement of Tire Brake Force Characteristics as Related to Wheel Slip Control System Design*", *SAE Trans., Vol.78, No. 690214, 1969, pp.909 – 925.*
- [10] Hattwig, P. (1993). *Synthesis of ABS Hydraulic Systems. Technical Report 930509, Society of Automotive Engineers. Warrendale PA.*
- [11] Jiang, F. (2000). *A Novel Approach to a Class of Antilock Brake Problems. Cleveland State University: PhD Thesis.*

- [12] Jiang, F.(2000). *"An Application of Nonlinear PID Control to a Class of Truck ABS Problems," Proceedings of the (40)<sup>th</sup> IEEE Conference on Decision and Control, Orlando, pp. 516 – 521.*
- [13] John Y. Hung, Weibing Gao and James C. Hung, February 1993, *"Variable structure control: A survey," IEEE Transactions on Industrial Electronics, vol.40, no.1, pp.2 – 22.*
- [14] Kachroo P. (1994). *Vehicle Traction Control and its Application. The University of California at Berkeley: Ph.D Thesis.*
- [15] K.D. young, V.I. Utkin and U. Ozguner,(1999), *"A control Engineer's guide to sliding mode control, IEEE Transactions on Control System Technology, vol.7, pp.328 – 342.*
- [16] Layne, J.R. (1993). *Fuzzy Learning Control for Antiskid Braking System. IEEE Transaction on Control Systems. June: IEEE, 122 – 129.*
- [17] Madau, D. P., Yuan, F., Davis, L. I. and Feldkamp, L. A. (1993). *Fuzzy Logic Antilock Braking System for a Limited Range Coefficient of Friction Surface. IEEE Transaction. Dearborn, Michigan: IEEE, 883 – 888.*
- [18] Maier, M. and Muller, K. (1995). *ABS5.3: The New and Compact ABS 5 Unit for Passenger Cars. Technical Report 930757, Society of Automotive Engineers. Warrendale PA.*
- [19] Maisch, W., Mergenthaler W.D., and Sigi, A. (1993). *ABS5 and ASR5: The New ABS/ASR Family to Optimize Directional Stability and Traction. Technical Report 930505, Society of Automotive Engineers. Warrendale PA.*
- [20] Mauer, G.F. (1995). *A Fuzzy Logic Controller for an ABS Braking System. IEEE Transaction on Fuzzy System. 381 – 388.*
- [21] Petersen, I. (2003). *Wheel Slip Control in ABS Brakes Using Gain Scheduled Technology: Ph.D. Thesis.*
- [22] Raymond A. Decarlo, Stanislaw H.Zak and Gregory P. Matthews, March (1988). *"Variable structure control of non-linear multivariable system," Proceedings of IEEE, vol. 76, No.3, pp. 212 – 232.*
- [23] Slotine, J.-J.E. and Li, W. (1991). *Applied Nonlinear Control. Englewood Cliffs, NJ: Prentice-Hall.*
- [24] Taborek, J. J.(1957). *Mechanics of Vehicle. Cleveland, OH: Penton.*

- [25] Tan, H.S., Tomizuka, M. (1990). *Discrete-time Controller Design for Robust Vehicle Traction*. In *IEEE control systems magazine*. April. IEEE, 107 – 13.
- [26] Unsal, C., Kachroo, P. (1999). *Sliding mode measurement feedback control for antilock braking systems*. *IEEE Transactions on Control Systems Technology*, 7(2), 271 – 281.
- [27] Vadim I. Utkin, April (1977). "*Variable structure systems with sliding modes*", *IEEE Transactions on Automatic Control*, vol. AC-22, pp. 212 – 222.
- [28] Wang, W.Y., Chen, G.M. and Tao, C.W. (2003a). *Stable Anti-Lock Braking System Using Output-Feedback Direct Adaptive Fuzzy Neural Control*. *IEEE. Transaction on System Man and Cybernetics*. IEEE, 3675 – 3680.
- [29] Wellstead, P. E. and Pettit, N. (1997). *Analysis and Redesign of an Antilock BrakeSystem Controller*. In: *IEE Proceedings of Control Theory Application*. IEE, 413 – 426.
- [30] Wong, J. Y.(1978). *Theory of Ground Vehicles*. New York: Wiley.

# Appendix

## Appendix A: Sample MATLAB Code

### [% SMC based ABS of a vehicle simulation initialization code](#)

```
function Xdot = smcneww(t,X)
%input initial state conditions
Xdot = zeros(4,1);
V = X(1);           \% Linear Velocity of the vehicle.
Ww = X(2);          \% Angular Velocity of the Wheel.
S = X(3);           \% Sliding surface
Lamda = X(4);       \% wheel slip
Rw = 0.326;         \% radius of the wheel.
Mup = 0.2;          \% peak value of the adhesion coefficient.
Lamdap = 0.15;     \% peak value of the wheel slipe.
Rho = 1.184;        \% air density.
Cd = 0.36;          \% aerodynamic drag coefficient.
Af = 3.03705;       \% frontal area of the vehicle(in meter square).
L = 2.985;          \% wheel base (meter).
m = 2550;           \% Total mass of the Vehicle(in killogram).
mt = 637.5;         \% mass of quarter vehicle (in killogram).
Hcg = 0.46;         \% center of gravity height (in meter).
Nw = 4;             \% total number of wheel during braking.
g = 9.81;           \% gravitational acceleration (in meter per second square).
Jw = 3;             \% moment of inertia of the wheel.
\% angular velocity of the vehicle
Wv = V/Rw;
W = max (Wv,Ww);
Mul = (2*Lamda*Mup*Lamdap)/(Lamdap^2 + Lamda^2);           \% adhesion coefficient
Fv = (Rho*Cd*Af*V^2)/8;                                     \% wind or aerodynamic drag force
```

```

\% acceleration of the vehicle {the derivative of vehicle velocity}
acc = (2*L/(2*m*L - Nw*Mul*m*Hcg))*(Nw*Mul*mt*g - Fv);
\% longitudinal weight transfer load due to braking
F1 = (m*Hcg*acc)/(2*L);
\% normal load
Nv = (mt*g) + F1;
\% Tractive force
Ft = Mul*Nv;
\% wheel viscous friction
Fw = 0.2*2550*9.81;
\% control signal derivation
b1 =(Nw*Nv)/(Rw*m);
b2 =(Rw*Nv)/Jw;
b3 =1/Jw;
f1 = Fv/(Rw*m);
f2 = (Rw*Fw)/Jw;
x1dot = - f1 + b1*Mul;
Ueq = (f2 + b2*Mul + (1 + Lamda)*x1dot - 0.83*Wv*(Lamda + 0.15))/b3;
Uc = Wv*sign(S);
U = Ueq - Uc;
\% angular acceleration of the wheel
angacc = b3*U - f2 - b2*Mul;
\% derivative of wheel slip
Lamdaderivative = (angacc - (1 + Lamda)*x1dot)/Wv;
\% derivative of the sliding surface
Sderivative = (1/0.83)*Lamdaderivative + (Lamda + 0.15);
\%state equation calculations
Vdot = acc;
Wwdot = angacc;
Sdot = Sderivative;
Lamdadot = Lamdaderivative;
\%convert back to Xdot matrix
Xdot=[Vdot; Wwdot; Sdot; Lamdadot];

```

**% SMC based ABS of a vehicle simulation running code**

```

\% initial conditions
V0 = 41.667;           \% for the initial velocity of 150 km per hour. this should
Ww0 = 127.8;          \% initially velocity of the wheel and the vehicle are equal
S0 = 0.15;            \% initial value of the sliding surface
Lamda0 = 0;           \% initial value of the wheel slip

\% time conditions
time = [0:0.01:22.23];
[t,X] = ode45(@smcneww,time,[V0; Ww0; S0; Lamda0]);
\%extract plot information from ode45 execution
V = X(:,1);
Ww = X(:,2);
S = X(:,3);
Lamda = X(:,4);

Rw = 0.326;           \% radius of the wheel.
Mup = 0.2;            \% peak value of the adhesion coefficient.
Lamdap = 0.15;        \% peak value of the wheel slipe.
Rho = 1.184;          \% air density.
Cd = 0.36;            \% aerodynamic drag coefficient.
Af = 3.03705;         \% frontal area of the vehicle(in meter square).
L = 2.985;            \% wheel base (meter).
m = 2550;              \% Total mass of the Vehicle(in killogram).
mt = 637.5;           \% mass of quarter vehicle (in killogram).
Hcg = 0.46 ;          \% center of gravity height (in meter).
Nw = 4;               \% total number of wheel during braking.
g = 9.81;             \% gravitational acceleration (in meter per second square).
Jw = 3;               \% moment of inertia of the wheel.

\% angular velocity of the vehicle
Wv = V./Rw;
W = max (Wv,Ww);
\%Lamda = (Ww - Wv)./W;           \% wheel slip
Mul = (2*Lamda.*Mup.*Lamdap)./(Lamdap.^2 + Lamda.^2);   \% adhesion coefficient
Fv = (Rho*Cd*Af*V.^2)/8;         \% wind or aerodynamic drag force
\% acceleration of the vehicle {the derivative of vehicle velocity}
acc = (2*L./(2*m*L - Nw*Mul*m*Hcg)).*(Nw*Mul.*mt*g - Fv);

```

```

\% longitudinal weight transfer load due to braking
F1 = (m*Hcg*acc)./(2*L);
\% normal load
Nv = (mt*g) + F1;
\% Tractive force
Ft = Mul.*Nv;
\% wheel viscous friction
Fw = 0.2*2550*9.81;
\% control signal derivation
b1 =(Nw*Nv)./(Rw*m);
b2 =(Rw*Nv)/Jw;
b3 =1/Jw;
f1 = Fv/(Rw*m);
f2 = (Rw*Fw)/Jw;
x1dot = - f1 + b1.*Mul;
Ueq = (f2 + b2.*Mul + (1 + Lamda).*x1dot - 0.83*Wv.*(Lamda + 0.15))/b3;
Uc = Wv.*sign(S);
U = Ueq - Uc;
angacc = b3*U - f2 - b2.*Mul;\% angular acceleration of the wheel
Lamdaderivative = (angacc - (1 + Lamda).*x1dot)./Wv;\% derivative of wheel slip
Sderivative = (1/0.83)*Lamdaderivative + (Lamda + 0.15);\% derivative of the sliding
\% angular acceleration of the wheel
\% stopping distance
x0 = 0;
x = x0 + (V0.*t) + (0.5*acc.*t.^2);
Vw = Ww*Rw; \% velocity of the wheel
[t V Vw x Lamda]
Tb = m*Rw.*acc;
U + Tb;
plot(t,V,'g',t,Vw,'r')    \%plots
grid
xlabel('time (second)'),ylabel('speed (m/s)')\

```